

# Dissolved organic carbon, major and trace elements in peat pore water of sporadic, discontinuous and continuous permafrost zone of Western Siberia

Tatiana V. Raudina<sup>1</sup>, Sergey V. Loiko<sup>1</sup>, Artyom G. Lim<sup>1</sup>, Ivan V. Krickov<sup>1</sup>, Liudmila S. Shirokova<sup>2,3</sup>, Georgy I. Istigechev<sup>1</sup>, Daria M. Kuzmina<sup>1</sup>, Sergey P. Kulizhsky<sup>1</sup>, Sergey N. Vorobyev<sup>1</sup>, Oleg S. Pokrovsky<sup>2\*</sup>

<sup>1</sup> BIO-GEO-CLIM Laboratory, Tomsk State University, Lenina av., 36, Tomsk, Russia

<sup>2</sup> GET UMR 5563 CNRS University of Toulouse (France), 14 Avenue Edouard Belin, 31400 Toulouse, France

<sup>3</sup> N. Laverov Federal Center for Integrated Arctic Research, Russian Academy of Science, Arkhangelsk, Russia

*Correspondence to:* Oleg S. Pokrovsky (oleg.pokrovsky@get.omp.eu)

**Abstract.** Mobilization of dissolved organic carbon (DOC) and related trace elements (TE) from the frozen peat to surface waters in the permafrost zone is expected to enhance under on-going permafrost thaw and active layer thickness (ALT) deepening in high latitude regions. The interstitial soil solutions are efficient tracers of on-going bio-geochemical processes in the critical zone and can help to decipher the intensity of carbon and metals migration from the soil to the rivers and further to the ocean. To this end, we collected, across a 640-km latitudinal transect of sporadic to continuous permafrost zone of western Siberia peatlands, soil porewaters from 30-cm depth using suction cups and we analyzed DOC, DIC and 40 major and TE in 0.45- $\mu$ m filtered fraction of 80 soil porewaters.

Despite an expected decrease of the intensity of DOC and TE mobilization from the soil and vegetation litter to the interstitial fluids with the increase of the permafrost coverage, decrease in the annual temperature and ALT, the DOC and many major and trace element did not exhibit any distinct decrease in concentration along the latitudinal transect from 62.2°N to 67.4°N. The DOC demonstrated a maximum of concentration at 66°N, on the border of discontinuous/continuous permafrost zone, whereas the DOC concentration in peat soil solutions from continuous permafrost zone was equal or higher than that in sporadic/discontinuous permafrost zone. Moreover, a number of major (Ca, Mg) and trace (Al, Ti, Sr, Ga, rare earth elements (REEs), Zr, Hf, Th) elements exhibited an increasing, not decreasing northward concentration trend. We hypothesize that the effect of temperature and thickness of the ALT are of secondary importance relative to the leaching capacity of peat which is in turn controlled by the water saturation of the peat core. The water residence time in peat pores also plays a role in enriching the fluids in some elements: the DOC, V, Cu, Pb, REE, Th were a factor of 1.5 to 2.0 higher in mounds relative to hollows. As such, it is possible that the time of reaction between the peat and downward infiltrating waters essentially controls the degree of peat pore-water enrichments in DOC and other solutes. A two-degree northward shift in the position of the permafrost boundaries may bring about a factor of  $1.3 \pm 0.2$  decrease in Ca, Mg, Sr, Al, Fe, Ti, Mn, Ni, Co, V, Zr, Hf, Th and REE porewater concentration in continuous and discontinuous permafrost zones, and a possible decrease in DOC, SUVA, Ca, Mg, Fe and Sr will not exceed 20% of their current values. The projected increase of ALT and vegetation density, northward migration of the permafrost boundary, or the change of hydrological regime are unlikely to modify chemical composition of peat pore water fluids larger than their natural variations within different micro-landscapes, i.e., within a factor of 2. The decrease of DOC and metal delivery to small rivers and lakes by peat soil leachate may also decrease the overall export of dissolved components from continuous permafrost zone to the Arctic Ocean. This challenges the current paradigm on the increase of DOC export from the land to the ocean under climate warming in high latitudes.

## 41 1 Introduction

42 Boreal and subarctic regions of the Northern Hemisphere are among the most vulnerable areas to on-going  
43 climate warming (Natali et al., 2011, 2015; Schuur et al., 2015; Vonk et al., 2015b; Pries et al., 2016). Because of  
44 sizeable carbon storage in frozen soils of Siberia (Botch et al., 1995; Kremetski et al., 2003; Frey and Smith, 2007;  
45 Beilman et al., 2009; Tarnocai et al., 2009; Gentsch et al., 2015), the warming in this region is especially important for  
46 global projections of the carbon balance on the planet (Smith et al., 2004; Frey and Smith, 2005; Feng et al., 2013). In  
47 this regard, permafrost-bearing part of Western Siberia Lowland (WSL) is highly sensitive to soil warming, due to (i) the  
48 dominance of discontinuous, sporadic and intermittent permafrost coverage compared to continuous and discontinuous  
49 permafrost of central and eastern Siberia and Canada High Arctic; (ii) the surface layer temperature of the WSL  
50 permafrost is often between 0 and -2°C, which is warmer than in other regions of the world (Romanovsky et al., 2010);  
51 (iii) essentially flat area of the WSL and high impact of flooding and thermokarst development, and most importantly (iv)  
52 high stock of ancient and recent organic carbon in the form of partially frozen peat deposits of 1 to 4 m thickness.

53 Mobilization of dissolved organic and inorganic carbon (DOC and DIC, respectively) and related trace elements  
54 (TE) including metal contaminants and micronutrients from the frozen peat to surface waters and further to the Arctic  
55 Ocean is one the major consequences of on-going permafrost thaw (Tank et al., 2012a, b, 2016; Striegl et al., 2005;  
56 Rember and Trefry, 2004; Prokushkin et al., 2011; Mann et al., 2012; Grosse et al., 2016; Holmes et al., 2013). The  
57 impact of warming on arctic and subarctic soil is primarily through the active layer thickness (ALT) rise (Zhang et al.,  
58 2005; Akerman and Johannson, 2008) although a number of other phenomena (plant productivity, drainage and  
59 hydrological regime change, ground fires etc) may be even more important in changing the biogeochemical cycle of  
60 carbon and metals in permafrost-affected soils (Jorgenson et al., 2013). For these reasons, the peat land zones have  
61 received significant attention (Haapalehto et al., 2011; Olefeldt and Roulet, 2012; Charman et al., 2013; Quinton and  
62 Baltzer, 2013; Muller et al., 2015; Morison et al., 2017), notably via natural manipulation experiments in order to assess  
63 the responses of peat carbon to simulated warming and oxidizing (Dielman et al., 2016; Liu et al., 2016), water table  
64 manipulation (Blodau and Moore, 2003; Strack et al., 2008; Goldberg et al., 2010) and drought (Clark et al., 2012).

65 The majority of available studies addressed the carbon and element transformation in the permafrost regions via  
66 analysis of rivers (Lobbés et al., 2000; Striegl et al., 2005; Spencer et al., 2008, 2015; Holmes et al., 2012; Wickland et  
67 al., 2012; Giesler et al., 2014; Mann et al., 2015), lakes (Kokelj et al., 2005, 2009; Guo et al., 2007; Laurion et al., 2010;  
68 Tank et al., 2009), mires (Olefeldt and Roulet, 2012; Olefeldt et al., 2013, 2014) or soil organic matter (SOM) from  
69 various depth and soil aqueous leachate (Swindles et al., 2015; Hodgkins et al., 2014, 2016; Drake et al., 2015; Vonk et  
70 al., 2015a; Yang et al., 2016) and largely ignored soil porewater chemistry. At the same time, interstitial soil solutions are  
71 known to be efficient tracers of on-going bio-geochemical processes in the critical zone (Hendershot et al., 1992; Stutter  
72 and Billett, 2003; Quinton and Pomeroy, 2006; Karavanova and Malinina, 2007; Gangloff et al., 2016) and can help to  
73 decipher the intensity of carbon and metals migration from the soil to the rivers and further to the ocean. However, in  
74 contrast to significant number of in-situ measurements of DOC and metals in the interstitial soil solutions of the boreal  
75 zone (Van Hees et al., 2000a, b; Reynolds et al., 2004; Starr and Ukonmaanaho, 2004; Michalzik et al., 2001; Giesler et  
76 al., 2006; Ilina et al., 2014; Griffiths and Sebestyen, 2016; Shotyky et al., 2016) there are relatively few studies of soil  
77 porewaters from the permafrost regions (e.g., Marlin et al., 1993; Prokushkin et al., 2005; Pokrovsky et al., 2006, 2013;  
78 Koch et al., 2013; Jessen et al., 2014; Fouche et al., 2014; Fouché et al., 2014; Mavromatis et al., 2014; Herndon et al.,  
79 2015), none of them dealing with organic-rich peatland soils. Only recently, Frey et al. (2016) reported results soil pore  
80 waters from the yedoma wetland soil within the flow-path continuum from the soil to the Kolyma River mainstream.

81 In this work we sampled, across a 640-km latitudinal transect of sporadic to continuous permafrost, the  
82 interstitial soil solutions of the largest peatland of the world. Our main goal was to quantify the distribution of DOC,  
83 major **and TE** in pore waters along a permafrost gradient of similar micro-landscapes. Within the upper unfrozen peat  
84 horizon, we hypothesize a trend of diminishing DOC and metal concentration northward, due to the decrease of mean  
85 annual temperature, vegetation density and active layer thickness. We aimed at quantifying the latitudinal trend of peat  
86 pore water concentration of DOC, major **and TE** and testing the difference in solute concentration sampled from various  
87 micro-landscape such as mound, hollow, depression, and polygon. Implying a substituting-space-for-time approach,  
88 developed for surface waters of western Siberia, (i.e., Frey et al., 2007a, b; Frey and Smith, 2005), the obtained results  
89 should allow a straightforward empirical provisions of soil water chemistry change during northward migration of the  
90 permafrost boundary. Because the main **source to** inland waters in this vast territory (over 1 million km<sup>2</sup>) occurs as supra-  
91 permafrost flow over the impermeable frozen peat horizon (Novikov et al., 2009), and due to the fact that the West  
92 **Siberian peatlands contain the largest soil water and ice resources in the northern hemisphere (Smith et al., 2012)**, the  
93 assessment of soil peat water chemical composition should help predicting the possible change of DOC and metal  
94 transport of permafrost-bearing Siberian rivers and lakes under climate warming scenarios.

95

## 96 **2. Materials and Methods**

### 97 **2.1. Geographical setting and local micro-landscapes**

98 Western Siberia Lowland (WSL) includes the watershed of the Ob, Pur, Nadym, Poluy and Taz rivers that drain  
99 Pleistocene sands and clays, covered by thick (1 to 3 m) peat. All three major zones of the boreal biome, taiga, forest-  
100 tundra and tundra, can be found in this region. The territory investigated in this work includes 3 main permafrost zones:  
101 sporadic, discontinuous and continuous (Fig. 1). Quaternary clays, sands, and alevrolites underlying the surface peat  
102 deposits range in thickness from several meters to 200-250 m and have fluvio-glacial and lake-glacial origin in the north  
103 of 60°N. The climate is humid semi-continental with mean annual temperature (MAT) ranging from - 2.8°C in the south  
104 of the cryolithozone (Syrgut region) to -9.1°C in the north (Tazovsky). **The annual precipitation ranges from 600 mm in**  
105 **Kogalym to 360 mm in Tazovsky**. Along the gradient of discontinuous to sporadic to continuous permafrost zone, we  
106 selected 5 main test sites whose physico-geographical characteristics are given in **Table 1**.

107 A typical feature of the WSL is the presence of positive and negative forms of relief – microlandscapes. **The**  
108 **initial bog with weakly pronounced micro-relief was subjected to freezing during Subboreal period (~ 4500 y.a). During**  
109 **Subatlantic period (2500 y.a.) and the increase of temperature and precipitation, the thermokarst started. The hollows**  
110 **received sufficient water and they started to thaw, whereas the mounds were rising due to ice wedges underneath (Panova**  
111 **et al., 2010; Ponomareva et al., 2012; Pastukhov et al., 2016)**. The positive forms include ridges in permafrost-free and  
112 sporadic permafrost zone, mounds in discontinuous permafrost zones, and polygons in the subarctic tundra of continuous  
113 permafrost. The negative forms comprise hollows (abundant across all zones), permafrost subsidences in discontinuous  
114 and continuous permafrost zones, and frost cracks of the polygonal tundra biome. In each of five major sites, several  
115 micro-landscapes corresponding to one positive and two negative form of relief were selected as specified in **Table 1** and  
116 shown as aerial views in **Fig. 1**. The cross sections of dominant micro-landscapes with corresponding soil specifications  
117 are represented in **Fig. 2** and include: (i) peat mounds in the 4 southern sites of flat mound peat bog, and corresponding  
118 polygon in the most northern, **Tazovsky** site of polygonal tundra; (ii) hollows in all 5 sites, and (iii) permafrost

119 subsidences in 4 southern sites and corresponding frost crack in Tazovsky. Typical soil profiles of studied sites are  
120 illustrated in **Fig. S1** of Supplement.

121

## 122 **2.2. Soil porewater sampling**

123 Altogether, 80 soil porous waters in 5 main sampling sites were collected in the end of July-beginning of August 2015. In  
124 this study, suction cup lysimeters were used. The chemical composition of interstitial soil solution is known to depend on  
125 the extraction method (e.g., Geibe et al., 2006; Schlotter et al., 2012). Detailed comparison between suction cup and press  
126 technique is described in methodological work of our group (Raudina et al., 2016). In the peat profile of each  
127 microlandscape, the PTFE suction cup lysimeters (95 mm long and 21 mm diameter, 2  $\mu\text{m}$  pore size) of SDEC (France)  
128 were installed at the depth of  $30\pm 15$  cm below the moss layer (**Fig. S2** of Supplement). The choice of the sampling depth  
129 was determined by the position of the permafrost table: typically, the cup was installed at 10 cm from the peat outcrop  
130 vertical surface, 5-10 cm above the bottom of the active layer, but not deeper than 40-50 cm from the moss layer. In all  
131 sites, the cups were installed exclusively in soils that belonged to group Histosols (according to WRB 2014, i.e., having a  
132 thickness of peat > 60 cm). The cups were connected via PTFE tubing to polypropylene 1-L container maintained at 75  
133 to 50 kPa via a Mityvac MV8255 PVC-made hand pump or a portable electric vacuum pump (KNF Neuberger W/VAC.  
134 5.5 L). Before each installation, the suction cups were cleaned by flushing with Milli-Q water (~ 250 mL), followed by  
135 3% ultrapure  $\text{HNO}_3$  (~ 250 mL) and finally Milli-Q water (~ 750 mL). Each cup was soaked in Milli-Q water for at least  
136 1 day before the experiment and was used only once. The porewater was collected in two steps. The first portion (100-  
137 200 mL) was collected during 24 h and the fluid was discarded, allowing for the saturation of the tubing and the recipient  
138 bottle surface. The 2<sup>nd</sup> portion (100-300 mL) was collected during the next 24 h of deployment or, in case of dryer  
139 conditions, over 48 h and used for analyses. The vacuum in the recipient bottle decreased from 75 kPa to atmospheric  
140 pressure over 24 h, and the first portion of the fluid appeared at 45 to 50 kPa.

141

## 142 **2.3. Analyses**

143 Collected waters were immediately filtered in pre-washed 30-mL PP Nalgene® flacons through single-use  
144 Minisart filter units (Sartorius, acetate cellulose filter) having a diameter of 25 mm and a pore size of 0.45  $\mu\text{m}$ . The first  
145 20 mL of filtrate were discarded. Filtered solutions for cation analyses were acidified (pH ~ 2) with ultrapure double-  
146 distilled  $\text{HNO}_3$  and stored in pre-washed HDPE bottles. The preparation of bottles for sample storage was performed in a  
147 clean bench room (ISO A 10,000). Blanks were performed to control the level of pollution induced by sampling and  
148 filtration. The DOC blanks of MilliQ filtrate never exceeded 0.1 mg/L which is quite low for the organic-rich pore waters  
149 sampled in this study (i.e., 10–100 mg/L DOC). pH was measured in the field using a combined electrode with un-  
150 certainty of  $\pm 0.02$  pH units. DOC and DIC were analyzed using a Carbon Total Analyzer (Shimadzu TOC VSCN)  
151 with an uncertainty better than 3%. The instrument was calibrated for analysis of both form of dissolved carbon in  
152 organic-rich, DIC-poor waters (e.g., Prokushkin et al., 2011). The UV absorbance of the filtered samples was measured  
153 at 280 nm using quartz 10-mm cuvette on Cary-50 spectrophotometer. The specific UV-absorbency ( $\text{SUVA}_{280}$ ,  $\text{L mg}^{-1} \text{m}^{-1}$ )  
154 is used as a proxy for aromatic C, molecular weight and source of DOM (Uyguner and Bekbolet, 2005; Weishaar et al.,  
155 2003; Ilina et al., 2014 and references therein). The  $\text{SUVA}_{280}$  in the present study was used for consistency with previous  
156 measurements of lakes and rivers in western Siberia (Shirokova et al., 2013; Manasyrov et al., 2015, 2017; Pokrovsky et  
157 al., 2015) and permafrost-draining rivers in Central Siberia (Prokushkin et al., 2011).

158 Major anions ( $\text{Cl}^-$ ,  $\text{SO}_4^{2-}$ ) concentrations were measured by ion chromatography (HPLC, Dionex ICS 2000) with  
159 an uncertainty of 2%. Major cations (Ca, Mg, Na, K), Si and ~40 TE were determined with an ICP-MS Agilent ce 7500  
160 with In and Re as internal standards and 3 various external standards, placed each 10 samples in a series of river water.  
161 Details of TE analyses in DOC-rich waters of western Siberia are given elsewhere (Pokrovsky et al., 2016a, b). The  
162 SLRS-5 (Riverine Water Reference Material for Trace Metals certified by the National Research Council of Canada) was  
163 used to check the accuracy and reproducibility of each analysis (Yeghicheyan et al., 2013). Only the elements that  
164 exhibited good agreement between replicated measurements of SLRS-5 and the certified values (relative difference <  
165 15%) are reported in this study.

166

## 167 2.4. Statistical treatment

168 The concentrations of carbon and major elements in soil porewaters were treated using the least squares method and  
169 Pearson correlation (SigmaPlot version 11.0/Systat Software, Inc). Regressions and power functions were used to  
170 examine the relationships between the elemental concentrations and the latitude of sampling. The normality of data  
171 distribution was checked using the criterion of Kolmogorov-Smirnov, separately for each site and for the full set of the  
172 data. The significance value was < 0.01 and thus non-parametric criteria for data comparison were used. First, major and  
173 TE concentrations in soil porewaters of (1) five main sampling sites and (2) four main micro-relief landscapes (polygon,  
174 permafrost/subsidence, frost crack and hollow) were processed using non-parametric H-criterion Kruskal-Wallis test.  
175 This test is suitable for evaluation of difference of each component among several samplings simultaneously. It is  
176 considered statistically significant at  $p < 0.05$ . In case of significant differences, a comparison of DOC, major and TE  
177 concentration between soil porewaters sampled in 3 main pair micro-landscapes (mound-hollow, mound-subside, and  
178 hollow-subside) of each 5 major sampling site was conducted using non-parametric pair Wilcoxon-Mann Whitney  
179 test. All graphics were performed using MS Excel 2010 and GS Grapher 11 package. Principal component analysis  
180 (PCA) was used for the full set of sampled soil porewaters across the micro-landscapes and permafrost zones. In this  
181 treatment, the main numerical variables were the geographic latitude of the sampling site, the depth of peat horizon,  
182 ALT, specific conductivity, pH, DOC, DIC, Cl,  $\text{SO}_4$ , Si, all major cations and 43 TE concentration.

183 The PCA analysis allowed to test the influence of various parameters, notably the latitude and the ALT on the soil  
184 porewater DOC and element variability. All the variables were normalized as necessary in standard package of  
185 STATISTICA-7 (<http://www.statsoft.com>) given that the units of measurements of various components are different.  
186 The identification of factors was performed using the method of Raw Data and the extraction method was principal  
187 component. The scree test involved plotting the eigenvalues in descending order of their magnitude against their factor  
188 numbers and determining where they level off. The PCA values demonstrated significant decrease of the value between  
189 F2 and F3 suggesting therefore that at least two factors are interpretable.

190

191

## 192 3. Results

### 193 3.1. PCA analysis and correlations between elements

194 The PCA analysis of all micro-landscapes and geographical zones yielded 2 possible factors contributing to  
195 observed variations in element concentration (i.e., 20 and 9%, Fig S3 (A, B) of Supplement). Such relatively low  
196 proportion of the variance explained by PCA is consistent with previous treatments of the WSL river water, conducted on  
197 a much larger dataset (Pokrovsky et al., 2016a). Because the standard STATISTICA-7 package used in this work does

198 not allow realization of Kaiser-Meyer-Olkin (KMO) criterion, we computed this criterion using Excel®. The KMO value  
199 was equal to 0.533 which suggests rather low adequacy: the analysis does not make sense at  $KMO < 0.5$ . Note that the  
200 removal a part of the data series and conducting separate PCA for major elements, TE, various forms of micro-relief and  
201 various geographical sites did not yield any better description of the variance mainly because of insufficient size of the  
202 dataset.

203 The first factor explains a greater variance in heavy element hydrolysates such as REEs, Cr, Nb, Zr, Hf, Th and  
204 U whereas the second factor was pronounced for soluble and biogenic elements (Mn, Co, Ni, V, Si, Ca, Mg, Sr), pH and  
205 latitude but also included Al and Fe, presumably due to organic complexation (see section 4.2 below). The correlation  
206 matrix (Table S1 of Supplement) and respective dendrogram of a hierarchical cluster for scaled pore water score  
207 variation (Fig. S3 C) demonstrated pronounced link of Si with REEs, Zr, Nb, Fe, Cr, V and Li, probably corresponding  
208 to the source of these elements from silicate matrix of the peat profile. There was positive correlation between Mn and Ca  
209 and Sr and Ca, reflecting the biological impact or soluble carbonate minerals as it is established for riverwater of the  
210 region (Pokrovsky et al., 2016a). Note that the correlations of latitude, specific conductivity, pH and DOC with all major  
211 and TE were poorly pronounced ( $R < 0.5$ ), whereas Fe and Al correlated with Si, Ti, V, Cr, Co, Ni, As, Zr, heavy REE,  
212 Hf.

213

### 214 3.2. Effect of micro-landscape

215 The mean values with S.D. of all major and TE in soil porewaters of main microlandscapes in each site are  
216 listed in Table 2. The mean values for the whole WSL territory for two dominant micro-landscapes, mound and hollow,  
217 are given in the last two columns of this table. Results of the application of Wilcoxon-Mann Whitney test for assessing  
218 the differences of DOC and several major and TE mean values between the dominant micro-landscapes in each site are  
219 listed in Table S2 of Supplement. According to the chosen statistical criteria, only a few elements (DOC, Al, Fe, Si, Mn,  
220 Cu, Cd, Pb, Hf, U) depicted significant differences in their concentration between different micro-landscapes. The DOC  
221 was approximately twice higher ( $p = 0.023$  to  $0.043$ ) in mounds (or polygons) compared to hollows in all 4 sites except  
222 Pangody, where the difference was only a factor of 1.1 which is not significant ( $p = 0.082$ ). In Khanymey, Urengoy and  
223 Tazovsky, the order of DOC concentration in various micro-landscapes was (mound or polygon)  $\geq$  (permafrost  
224 subsidence or frost crack)  $>$  hollow. Cu and, sometimes, Zn, followed this order. Concentrations of Al, Si, Fe, Sr did not  
225 demonstrate any systematic difference between positive and negative forms of relief for each site, without distinct  
226 preferential enrichment of one microlandscape versus another in the north or in the south. The minimal contrast in DOC  
227 and element concentration between micro-landscapes was observed in Pangody and the maximal variability was in  
228 Khanymey.

229 Within the standard deviation of the mean values, there was no difference in DIC, Si, Ca and Mg concentration  
230 between different micro-landscapes in all studied sites. The exception was Khanymey where the hollows demonstrated a  
231 factor of 1.5-2.8 higher Mg, Si and Ca concentration compared to mounds and Urengoy where the mounds contained less  
232 Mg and Si than the hollows. However, in the latter case, at  $p = 0.041$  to  $0.048$ , this difference was within the variation of  
233 the average (Table S 2). The mean concentrations of DIC, Cl, K, Si, Ca, Mg, Al, Fe, Ti, Sr, Ba, Zn, Mn, Ni and TE over  
234 the full WSL territory are quite similar ( $\pm 20\%$ ) between positive and negative forms of relief (compare the last two  
235 columns of Table 2). The DOC, B, Na, V, Ga, Cu, Cs, Pb, REE and Th exhibited a factor of  $1.5 \pm 0.2$  (significant at  $p <$   
236  $0.05$ ) higher WSL-mean concentrations in mounds/polygons compared to hollows.

237

### 238 3.3. Effect of latitude and permafrost zone on peat porewater concentrations of DOC and metals

239 In order to examine the latitudinal trend of element concentration in the porewater, first we run the Kruskal-  
240 Wallis and then the Wilcoxon-Mann Whitney pair test for overall differences. After that we assessed, which micro-  
241 landscape exhibited the largest difference between sites. Results include the p-value of the difference between one given  
242 site and other sites located northward (Table S3 of the Supplement). The difference between sites was tested for  
243 mounds/polygons and hollows for all 5 sites and for permafrost subsidence/frost crack for 3 most northern sites  
244 (Khanymey, Urengoy and Tazovskiy). The DOC and major elements (Ca, K, Al, Si, Fe) exhibited clear difference ( $p <$   
245 0.05) between different geographic zones. The most pronounced difference between pair sites was observed for hollows.  
246 Thus, the porewaters from hollows in most southern site (Kogalym, of the sporadic permafrost) demonstrated statistically  
247 significant differences in DOC, Ca, K, Al, Si, Ni, Cu, Sr, Rb concentrations from hollows of Khanymey, Pangody,  
248 Urengoy, and Tazovskiy. Among the elements listed in Table 2, DOC, Ca, Fe and Sr were found to be most sensitive to  
249 the latitude of the sampling site regardless of the type of micro-landscape.

250 The general latitudinal trend in element concentration together with mean values in each micro-landscape as a  
251 function of latitude was examined for all major and TE. The latitudinal trend was approximated by a linear regression  
252 using all micro-landscapes and individually for hollows and mound/polygons:

$$253 \quad [\text{Element}] = A + B \times \text{Latitude } (^{\circ}\text{N}) \quad (1)$$

254 where  $A$  and  $B$  are the element-specific empirical coefficients. Parameters of equation for each element are listed in  
255 Table 3. For most major components including DOC there was no systematic trend of increasing or decreasing of  
256 average concentration across the 640 km latitudinal profile. There was a local maximum of DOC concentrations in  
257 porewaters of peat mounds sampled at the Khanymey-Urengoy sites. Overall, 3 patterns of concentration – latitude  
258 dependence could be distinguished shown in Figs. 3-5 and S4-S5:

259 (1) Specific Conductivity, pH, DIC, DOC, K, Na, SO<sub>4</sub>, Si, B, Li, Fe, Ti, Cr, Ba, Mo, As, light REEs (La, Ce), W, and U  
260 did not exhibit any statistically significant trend ( $R^2 < 0.5$ ) or this trend was within the uncertainties as illustrated in Fig.  
261 3 A-H and Fig. S4 E-K;

262 (2) A clear trend of steady increasing concentration northward was observed for SUVA<sub>280</sub>, Mg, Ca, Al, Cu, V, Mn, Ni,  
263 Sr, heavy REEs, Zr, Hf, Th ( $0.45 < R^2 < 0.62$ ,  $p < 0.05$ ). The overall increase from sporadic to continuous permafrost  
264 zone ranged from a factor of 2 to a factor of 5, illustrated in Fig. 4 A-H and Fig. S5 A-F.

265 (3) Cl, Sb, Pb, Cd, Zn, Rb, and Cs exhibited a decreasing trend northward shown in Fig. 5 A-E ( $0.48 < R^2 < 0.84$ ).

266 For some elements, there was a lack of any trend between 62°N and 66.5°N, followed by an increase (significant at  $p <$   
267 0.05) between 66 and 67.5°N: Ca (Fig. 4 C), Mn (Fig. S5 A), Co (Fig. S5 B), V (Fig. 4 F) and As (Fig. S4 H). The most  
268 pronounced trend of element concentration increase northward was observed in mounds/polygons for Al ( $R^2 = 0.91$ ), Sr  
269 ( $R^2 = 0.69$ ), Zr ( $R^2 = 0.57$ ), Ce ( $R^2 = 0.76$ ), Hf ( $R^2 = 0.68$ ) and Th ( $R^2 = 0.92$ ). For these elements, the trend in  
270 hollows/cracks was much less pronounced or even absent, with  $R^2 < 0.5$  (Table 3). A decreasing trend of element  
271 concentration northward was also better pronounced in mounds/polygons for Na, Cl, Rb, Cs and Pb.

272

## 273 4. Discussion

### 274 4.1. Dissolved organic carbon transport in peat soils

275 The first unexpected result of this study was the lack of significant decrease of DOC concentration in peat porewaters  
276 northward, from sporadic to discontinuous and continuous permafrost zone (Fig. 3 C). The character of the DOM also  
277 remained highly constant across the latitudinal / permafrost gradient as the SUVA<sub>280</sub> ranged from 2.4 to 3.5 L mg<sup>-1</sup> m<sup>-1</sup> in

278 all sites regardless of the microlandscape, with weak increase northward (**Fig. 4 A**). These values of SUVA<sub>280</sub> are  
279 consistent with those of the lakes (2 to 4 L mg<sup>-1</sup> m<sup>-1</sup>, Manasyrov et al., 2015) and rivers (2 to 3.5 L mg<sup>-1</sup> m<sup>-1</sup>, Pokrovsky  
280 et al., 2015) of the region during summer period. The previously published values of SUVA<sub>280</sub> in WSL surface waters  
281 were similar across a large scale of lake size (from 50 to 500,000 m<sup>2</sup>) and latitudinal position of the river watershed (from  
282 57°N to 66°N). This strongly suggests highly uniform feeding of Siberian inland waters by allochthonous DOM  
283 originated from peat leaching within the soil profile. The DOC transport to the river and lake presumably occurs via  
284 suprapermafrost flow over the frozen peat layers at the depth ranging between 20 and 80 cm depending on the season, the  
285 latitude and the micro-landscape context (see Fig. 2). Given the similarity of SUVA<sub>280</sub> values across significant  
286 geographical transect **on positive forms of micro-relief (Fig. 4 A, Table 3)**, we hypothesize the similarity of the nature of  
287 water-soluble OM that constitutes the peat **on mounds**. At the same time, **sizeable** increase in the SUVA<sub>280 nm</sub> northward  
288 may indicate a higher aromaticity of soil porewater DOM in the continuous permafrost zone relative to discontinuous and  
289 sporadic permafrost zone (Fig. 4 A). **The change of SUVA from 2.4 to 3.4 in hollows demonstrates a significant shift in**  
290 **the composition of the DOM and may have a pronounced effect upon the biogeochemical processing of DOM upon**  
291 **export as it has been recently shown in Eastern Siberia (Frey et al., 2016).** This contradicts the conclusion reached in  
292 recent studies of surface waters and soil leachates that the DOM leached from the permafrost soil layer has a consistently  
293 lower concentration of aromatic carbon (i.e. lower SUVA<sub>254</sub> values, Mann et al., 2012; Cory et al., 2013, 2014; Abbott et  
294 al., 2014; Ward and Cory, 2015), compared to DOM draining from the active, organic surface layer. However, the  
295 majority of previous studies dealt with non-peat permafrost environment. In the case of the WSL peatland, the  
296 contribution of UV-transparent microbial exometabolites and plant exudates including low molecular weight organic  
297 acids (i.e., Giesler et al., 2006) is certainly much higher in the southern forest-tundra and taiga zone compared to  
298 northern sites of the polygonal tundra. **In the present study, statistically significant increase of SUVA<sub>280</sub> northward in**  
299 **hollows (R<sup>2</sup> = 0.599, see Table 3) may also indicate the lower rates of DOM processing in soils in the north, linked to**  
300 **either shorter residence time of soil fluids or weaker processes of photo- and bio-degradation in continuous permafrost**  
301 **zone compared to sporadic and discontinuous zone.**

302 Generally higher DOC concentration in porewaters of mounds compared to that of hollows (Table 2) has two  
303 possible explanations. The soluble DOC retainment by clay horizon that underlays the peat in the WSL was  
304 hypothesized as the main regulator of the DOC level in rivers of large latitudinal transect of WSL, from permafrost-free  
305 to continuous permafrost zone (Pokrovsky et al., 2015). The gradient consisted in increasing the DOC concentration  
306 northward of 64°N (Pokrovsky et al., 2015) because the DOC-adsorbing clay horizon that underlays the peat may be  
307 frozen in the north (Kawahigashi et al., 2004). The latter authors suggested that the DOC in northern, permafrost-affected  
308 tributaries of the Yenisey River was less biodegradable (and thus better preserved during its transport from the soil to the  
309 river) than that in southern tributaries. If true, the lower DOC concentrations in hollows and subsidence relative to the  
310 mounds observed in the present study is due to DOC adsorption on unfrozen mineral layers (silt, clays) located below the  
311 peat horizon in depressions and hollows, which have much deeper position of the ALT than the mounds (see Table 1 and  
312 Fig. 2). At the same time, if soil pore waters are affected by the presence of minerals, then it should impact primarily the  
313 lithogenic elements (Ca, Mg, Sr, Si, Ti, Al, Zr...) whose concentration should be higher in negative forms of relief  
314 relative to that in the positive ones. This hypothesis is not supported by the concentration pattern of inorganic  
315 constituents of porewaters as shown in the next section. **Note also that, because the mounds thaw later than hollows, the**  
316 **period of unfrozen exchange of constituents in the soil with porewater is shorter in mounds compared to hollows.**



317 However, this does not go in line with the observed difference of higher DOC and metal concentration in porewater of  
318 mounds relative to hollows.

319 The 2<sup>nd</sup> explanation of the elevated DOC concentration in mounds compared to hollows across the whole  
320 permafrost gradient is related to the time of reaction between the peat and the pore fluids. From detailed hydrological  
321 studies on frozen peatbog of western Siberia, the water residence time in peat mound is a factor of 14 higher than that in  
322 hollows and depressions (Novikov et al., 2009). The latter have much higher hydrological connectivity to surrounding  
323 streams and temporary water channels and as such offer shorter contact time and pathways of vertically infiltrating and  
324 laterally migrating water. During the summer baseflow period, up to 70-80% of watershed covered by mounds in frozen  
325 peatland of western Siberia may remain disconnected from the hydrological network (Batuev, 2012). The mounds and  
326 polygons are therefore essentially controlled by water evaporation, leading to evaporative concentration of DOC and  
327 other solutes within the soil profile. The available data on water infiltration parameters of hollows and permafrost  
328 subsidences located in discontinuous permafrost zone of the WSL demonstrate an order of magnitude faster water  
329 migration in various depressions (hollows, subsidences) compared to mounds (Novikov et al., 2009 and unpublished data  
330 of the authors on NaCl tracer migration in frozen polygons and palsa peatbogs of the WSL). The density of the peat in  
331 the mounds and polygons is a factor of 2 to 10 higher than that in the hollows and depressions (Ivanov and Novikov,  
332 1976). Thus an analogy of ground surface and deep peat can be used for comparison between negative and positive forms  
333 of microrelief, respectively. In the peatland-dominated zone of discontinuous permafrost, the total porosity was reported  
334 to drop by about 10% between the ground surface and 35 cm depth; however, the active porosity decreased by as much  
335 as 40% over the same distance (Quinton et al., 2000). The saturated hydraulic conductivity of peat decreases rapidly with  
336 depth (Quinton et al., 2009). It thus can be hypothesized that, in the dense peat on mounds and polygons, the pores are  
337 significantly smaller with less interconnection, which leads to more restricted flow and greater tortuosity (Rezanezhad et  
338 al., 2009, 2010, 2016). All these factors should increase the water residence time in pores of peat in mounds relative to  
339 hollows and allow for efficient enrichment of peat porewater by DOC in the former.

340 The DOC pore water concentration invariance across the latitudinal gradient of the WSL is consistent with the  
341 lack of peat thickness and thermal regime effect on pore water chemistry. First, the peat thickness did not exert a direct  
342 impact on the degree of porewater enrichment in DOC among various micro-landscapes: there was no dependence  
343 between the DOC concentration in porewater and the total thickness of the peat ( $R^2 < 0.01$ , not shown). Second, the  
344 thermal regime of soil porewater is responsible neither for the difference between mounds and hollows nor for latitudinal  
345 dependence of DOC concentration. The effect of temperature on peat leaching in aqueous solution is not known, but by  
346 analogy with surface-controlled dissolution reaction of minerals (i.e., Schott et al., 2009) it can be by a factor of 2 to 3 for  
347 each 10°C rise. Such a large difference in 10°C between different adjacent micro-landscape seems highly unlikely. This  
348 is confirmed by both our field measurements in Tazovsky (mean annual temperature of peat at 5 cm depth is equal to -  
349 1.9°C in mound and +1.9°C in hollow), and the observations of other researchers in the WSL. In the Nadym region  
350 (discontinuous permafrost zone), the mean annual temperature of mounds and hollows is 1.0 and 1.6°C, respectively  
351 (Bobrik et al., 2015). At the latitude of Urengoy-Tazovsky and Khanymey, the average difference between mound and  
352 hollow of summer-time temperature at 20 cm depth is 2.9 and 3.4°C, respectively (Novikov et al., 2009). A similar  
353 difference of peat temperature between mounds and depressions at 20 cm depth ( $< 4^\circ\text{C}$ ) was reported for the Noyabrsk  
354 region (discontinuous permafrost zone, Makhatkov and Ermolov, 2015). Globally, the temperature of soil porewater  
355 across the latitudinal gradient does not exceed 10°C (Novikov et al., 2009) which is not sufficient to exert any  
356 pronounced control on DOC concentrations.

357 To summarize, we hypothesize that *i*) the DOC concentration should be controlled by the DOC residence time  
358 and travel pathway through the organic topsoil and *ii*) the enrichment in DOM of the interstitial soil solution occurs via  
359 lichens, moss, litter and peat leaching. Although the runoff is known to exert the primary control on stream DOC export  
360 from the boreal peatland catchments (Olefeldt et al., 2013; Leach et al., 2016), the existing hydrological modeling of  
361 subsurface transport of dissolved carbon in a discontinuous permafrost zone suggests that both concentration and load of  
362 DOC are water flow-independent (Jantze et al., 2013). As such, it is the time of reaction between the peat and downward  
363 infiltrating waters that essentially controls the degree of peat pore-water enrichments in DOC. This time is presumably  
364 similar across significant permafrost and climate gradients.

365

#### 366 **4.2. Factors controlling major and trace element concentration in peat soil porewaters**

367 Organic and organo-Fe, Al colloids dominate the speciation of most cations (including alkaline-earth metals)  
368 and TE in low-TDS humic surface waters of permafrost-affected WSL territory (Pokrovsky et al., 2016b), similar to  
369 other boreal catchments (Köhler et al., 2014). As a result, the behaviour of many major and TE in peat porewater is likely  
370 to follow that of DOC, Fe and Al as main colloidal carriers. The importance of colloidal Fe and Al as primary carriers of  
371 TE in peat soils is confirmed by results of this study: in pore-waters, none of the TE correlated with DOC ( $R < 0.5$ )  
372 whereas Fe and Al concentrations correlated with many TE such as Ti, V, Cr, Co, Ni, As, Sr, Zr, Nb, heavy REE, Hf.  
373 This is consistent with decoupling of  $TE^{3+}$  and DOC during size separation procedure as two independent colloidal pools  
374 (high molecular weight Fe, Al-rich and low molecular weight  $C_{org}$ -rich), already demonstrated for European boreal rivers  
375 (Neubauer et al., 2013; Vasyukova et al., 2010) and other Siberian rivers and WSL thermokarst lakes (Pokrovsky et al.,  
376 2006; Pokrovsky et al., 2011, 2016b). At the same time, although organo-ferric and organo-aluminium colloids are  
377 certainly important factors of insoluble element transport in peat soil, the source of TE may become more limiting for  
378 overall concentration of TE in soil porewater than their speciation. There are two possible sources of “lithophile”  
379 elements in the peat and peat porewaters: atmospheric dust deposition at the moss and lichen surface and upward  
380 migration of soil fluids that carry mineral particles from underlying loam horizons. The loam horizons are rich in silicate  
381 clay minerals (e.g., Ovchinnikov et al., 1973; Golovleva et al., 2017) that contain insoluble elements. The geochemical  
382 analysis of TE distribution in WSL peat cores across the studied permafrost gradient allowed to distinguish several  
383 categories of TE depending on their source such as soluble atmospheric aerosols, atmospheric dust, underlying mineral  
384 layers, plant biomass, and surface water flooding (Stepanova et al., 2015). The atmospheric deposition of lithogenic  
385 elements in the form of soluble aerosols on the moss surfaces followed by incorporation into the peat is expected to be  
386 low as shown by thorough snow analyses across the large WSL gradient (Shevchenko et al., 2016). Therefore,  
387 atmospheric dust seems to be the main source of insoluble metals in WSL peat as it is also known from other northern  
388 bogs (Shotyk et al., 2016). Regardless of the origin of lithophile elements, we hypothesize that the leaching of insoluble  
389 trivalent and tetravalent hydrolysates ( $TE^{3+}$ ,  $TE^{4+}$ ) from solid phase to interstitial soil solution may be restricted by the  
390 availability of silicate clay minerals within the peat core.

391 Based on results of the PCA treatment (Fig. S3 A, B), the dendrogram of a hierarchical cluster (Fig. S3 C) and  
392 the correlations between elements (Table S1) we hypothesize that the source of Cr, V, Al, REEs, Nb, Zr, Hf, Th, U but  
393 also of Mg and Li is silicate minerals dispersed within the peat matrix. These elements exhibit the highest correlation  
394 with Si in porewaters and appear to be linked to the first factor (F1) of the PCA. The silicate minerals may originate from  
395 both atmospheric dust and underlying clay/silt horizons. The lack of correlation of K, Rb, Mn, Ba, Mo, W, Zn, Pb, Cd,  
396 Cs, Sb with DOC, Fe or Al in peat porewaters of WSL (Table S1) can be explained by specificity of these elements. In

397 particular, K, Rb, Mn, Cu, Ba are biotically-controlled by moss growth and thus unlikely to be linked to any mineral  
398 source (Stepanova et al., 2015). It seems also plausible that indifferent oxyanions (Mo, Sb, W) or disperse pollutants  
399 delivered by atmospheric deposition on moss surface followed by incorporation into peat (Zn, Cd, Pb, Sb, Tl) do not  
400 exhibit significant correlation with main colloidal components.

401 One can expect that dissolved element decreases its concentration in the peat porewater northward regardless of  
402 the micro-landscape due to *i*) decrease of the thickness of peat deposits in total and the active soil (peat) layer in  
403 particular (Beilman et al., 2009; Novikov et al., 2009; Stepanova et al., 2015) which decreases the amount of peat  
404 interacting with downward penetrating fluids; *ii*) decrease of plant biomass (Frey and Smith, 2007), which diminishes the  
405 amount of plant litter that can release the elements (Pokrovsky et al., 2006; Fraysse et al., 2010), and also decrease the  
406 plant ability to weather minerals within the soil profile (Moulton et al., 2000); *iii*) shortening the unfrozen period of the  
407 year leading to the decrease of the residence time of water in soil pores and *iv*) overall decrease of the intensity of  
408 chemical weathering, CO<sub>2</sub> consumption and riverine fluxes with mean annual temperature decrease (Dessert et al., 2003).  
409 However, an unexpected result of this study was that the overwhelming number of major and TE did not exhibit any  
410 statistically significant decreasing trend of concentration with latitude. Instead, we observed a measurable northward  
411 increase in concentration of a number of lithogenic elements, whose presence is known to mark the intensity of mineral  
412 weathering. These are Mg, Al, Ti, V, Sr, REEs, Zr, Hf and Th, originated from silicate minerals of the soil profile. For  
413 example, Al, Ba, Fe, and Mn were reported to reflect the mineral weathering as they exhibited elevated concentrations in  
414 Alaskan rivers during the late Fall, that correlated with the maximal depth of the thawed active layer (Barker et al.,  
415 2014). The mechanism related to enhanced mobilization of low-soluble elements during deepening of the ALT is  
416 penetration of DOM-rich surface fluids to deeper soil horizon and leaching of lithogenic elements from underlying  
417 mineral substances, in the form of strong organic complexes (chelates). This mechanism can be tested via comparison of  
418 lithogenic element concentration in contrasting micro-landscapes. Thus, Sr, which is considered as an indicator of  
419 mineral sources in surface waters of the permafrost zone (Keller et al., 2010; Bagard et al., 2011), was highly similar  
420 between mound and hollow or even higher in mounds than in hollows or subsidences (Table 2). Given that the negative  
421 forms of relief in the WSL exhibit higher proximity of thawed layer to the mineral horizon because of lower thickness of  
422 peat and deeper ALT (Tyrtikov, 1973; Lupachev et al., 2016), the lack of link between Sr concentration and ALT  
423 position within the peat-silt/clay profile suggests that the underlying minerals do not participate in feeding the soil  
424 solutions by lithogenic elements. Rather, aeolian (long-range) dust deposits throughout the territory may lead to  
425 incorporation of solid atmospheric particles into the moss biomass. Subsequently, it is the dissolution of agglutinated  
426 minerals that enriches the peat porewater in lithogenic elements, including Si. Moreover, the concentration of elements  
427 likely originated from silicate matrix (Al, Si, Fe) in hollows and subsidences did not exceed that in mounds. Taken into  
428 account that the position of the permafrost boundary is much closer to the mineral substrate in negative forms of relief  
429 compared to mounds (see Table 1 and Fig. 2), this strongly suggests the lack of element leaching from the underlain  
430 mineral matrix. As such, the observed trends of element concentration with latitude reflect the leaching of essentially peat  
431 constituents with associated silicate particles without interferences with massive deposits of underlying sand, clay and silt  
432 in various micro-landscapes. Following the same reasoning, the lack of DIC, Mg and Ca variation among the micro  
433 landscapes suggests a negligible role of silicate and carbonate mineral weathering within the peat profile.

434 In addition to evaporative concentration mechanism and the greater residence time of solutes in mound  
435 compared to hollows, identified for DOC pattern in section 4.1, the peat chemical composition may be different between  
436 negative and positive forms of relief and thus it can contribute to porewater enrichment in major and TE. Indeed, the

437 degree of peat decomposition and elementary content of peat on mounds is higher than that on hollows and depressions  
438 (Stepanova et al., 2015): a comparison of peat elementary composition at 15 cm depth on Pangody site demonstrated a  
439 factor of 1.5 to 3.5 higher concentration in mounds compared to hollows of major (Ca, K, Na, Fe) and ~40 TE except  
440 Mg, Zn, Sb and Pb (a factor of 1.3 to 3 richer in hollows than in mounds).

441

442 The lack of increase of Cl, SO<sub>4</sub> and Na in peat porewaters from the most northern site (Tazovski) compared to  
443 the intermediate sites (Urengoy, Pandogy) dismisses the possibility of element leaching from frozen saline sediments  
444 abundant in the Russian Arctic Coast (e.g., Brouckov, 2002). Presumably, these saline sediments are not in contact with  
445 soil and suprapermafrost waters even at the time of maximal ALT, as also inferred from riverwater geochemistry in the  
446 permafrost-affected region of WSL (Pokrovsky et al., 2015). The elements originated from marine aerosols such as Na,  
447 Cl, SO<sub>4</sub>, B, Li, Rb, Cs exhibited a decreasing or indifferent, but not increasing trend of concentration northward. This  
448 precludes a strong influence of marine atmospheric deposition on surface water chemistry, unlike it was suggested in  
449 earlier works in this region (Syso, 2007; Smolyakov, 2000).

450

451

#### 452 4.3. Comparison of peat porewaters with rivers and thermokarst lakes

453 The peat soil porewaters sampled above the position of the permafrost table can serve as representative sources  
454 of water and solutes **prior to export to** the thermokarst lakes and rivers (Fig. 2). Therefore, a first-order comparison of  
455 concentrations between these aquatic systems allows evaluation of the role of peat (shallow surface) versus mineral (deep  
456 subsurface and underground waters) feeding of Siberian inland waters. This comparison was based on mean values of  
457 DOC and TE concentration in porewaters for the whole permafrost-affected WSL territory (Table 2) and those previously  
458 published for lakes and rivers of the same latitudinal gradient (Manasypov et al., 2014 and Pokrovsky et al., 2015,  
459 2016a). The dissolved components measured in rivers and lakes during summer period can be classified into three  
460 categories: (1) Rivers or lakes exceed soil porewaters by a factor of 3 to 10; (2) River or lakes are similar to porewaters  
461 within a factor of 2, and (3) Rivers or lakes are significantly lower (more than a factor of 3) than the porewaters. The  
462 elements of the first category are DIC, Ca, Mg, Si, B, Al, Mn, Na for rivers and only Si for lakes. The second category  
463 comprises DOC, Li, K, Rb, Fe, Ni, Co, Cr, As, Sr and U for rivers and Li, B, Na, K, Rb, Cs, Ca, Mg, Ti, V, Mn, Ni, Cu,  
464 Zn, Co, Cd, Sr, Mo, As, Sb for lakes. The 3<sup>rd</sup> category includes Ti, Cu, Pb, Cd, Mo and REEs for rivers and DOC, Al, Fe,  
465 Ga, Y, Zr, Ba, W, REEs, Th, U for lakes. This first-order comparison demonstrates that the soil porewaters alone are  
466 sufficient to provide the concentrations of all major and **TE** in lakes. In other words, the transport of soil porewaters  
467 along the permafrost boundary in the form of suprapermafrost flow may be the sole source of incoming solutes to  
468 thermokarst lakes of western Siberia, across all 3 permafrost zones. This hypothesis is fully consistent with the lack of  
469 any underground feeding of WSL thermokarst lakes, demonstrated in earlier studies (Manasypov et al., 2015).

470 In contrast to lakes that can be fully supplied by solutes from surrounding peat porewaters, the rivers require  
471 some “mineral” influx in addition to surface and shallow subsurface “organic” flux, in order to explain the elevated  
472 concentrations of DIC, Ca, Mg, Na, Si, Al in the riverwater relative to the peat porewater. This influx, mostly  
473 pronounced during summer baseflow period, may include the groundwater seeping via taliks on the river bed and shallow  
474 subsurface flow over clays and silt deposits. This process is fairly well known for other, non-peatland permafrost setting  
475 (MacLean et al., 1999; Bagard et al., 2011; Barker et al., 2014; Tank et al., 2016).

476 The latitudinal dependences of element concentration in the peat pore water revealed in this study can be  
477 compared to the latitudinal dependences of DOC and element concentration in adjacent thermokarst lakes and rivers. The  
478 elementary trends in the inland waters of western Siberia were associated to the influence of marine aerosols or long-  
479 range atmospheric transport of industrial pollutants in lakes (Manasypov et al., 2014) and the evolution of chemical  
480 composition of the peat and underlying mineral deposits in rivers (Pokrovsky et al., 2015; 2016a). However, the possible  
481 links are not straightforward and valid only for a small number of elements. Thus, increasing concentrations of Ca, Ni  
482 and Sr (**Fig. 4C, 4G, 4H**, respectively) and decreasing concentration of Sb and Pb (**Fig. 5 D and E**, respectively)  
483 northward are consistent with the trend in thermokarst lakes of western Siberia from 63°N to 71°N (Manasypov et al.,  
484 2014). However, the other elements exhibiting a clear increasing (K, Cu, Mo) or decreasing (V, Ba) latitudinal trend in  
485 lakes (Manasypov et al., 2014) do not show such a trend in peat pore-waters sampled in this study. Presumably, variable  
486 and simultaneously acting processes control the delivery of element from the peat core to the adjacent lakes over the  
487 permafrost gradient.

488 Because the leaching of peat constituents by downward penetrating fluids is very fast and weakly depends on  
489 temperature and local hydrological pathway within the peat pores, one can expect that the global hydrological setting will  
490 primarily control the peat weathering intensity. As such, it is the amount of water that passes through the peat soil  
491 column before being evacuated to the river that defines the overall export fluxes of elements from the peatland to the  
492 hydrological network. This prediction is consistent with reported higher riverine fluxes of DOC, Si and cations in the  
493 northern region of the WSL (66.5 to 67.5°N) relative to the southern region (62-65°N) of this territory corresponding to  
494 higher surface runoff in the north (Pokrovsky et al., 2015).

495 Today, the majority of Ca, Mg and  $\text{HCO}_3^-$  ions carried by rivers is used for calculation the  $\text{CO}_2$  uptake flux due  
496 to chemical weathering, i.e., reaction of atmospheric  $\text{CO}_2$  with Ca, Mg-bearing silicate minerals (Dessert et al., 2003;  
497 Beaulieu et al., 2012). Not more than 10% of total riverine flux of Ca, Mg and  $\text{HCO}_3^-$  is considered to be due to  
498 atmospheric input. An important consequence of our obtained results on soil porewaters in the WSL is that the intensity  
499 of chemical weathering and associated  $\text{CO}_2$  consumption in the permafrost regions (i.e., Beaulieu et al., 2012) by small  
500 rivers without pronounced underground feeding in peatlands could be overestimated relative to the regions with shallow  
501 organic soil horizons. As a result, the flux of DIC and major cations in the peatland-draining rivers should be corrected  
502 for the input of these elements via peat pore-water discharge to the river main stream. For a number of small rivers  
503 ( $S_{\text{watershed}} < 1000 \text{ km}^2$ ) in the permafrost zone of the WSL that are fed by shallow surface runoff through the peat horizon,  
504 this correction can range from 20 to 80% of total riverine DIC, Ca and Mg flux. The global consequence of this  
505 correction is that the continental-weathering  $\text{CO}_2$  sink in northern peatland regions might be a factor of 2 to 4 smaller  
506 than that currently deduced from the fluxes of large rivers.

507

508

#### 509 4.4. Prospective for climate change in western Siberia

510 In accordance with a common scenario of the climate change in the subarctic, a shift of the permafrost boundary  
511 further north and the increase of the active layer thickness are anticipated in the WSL (Pavlov and Moskalenko, 2002;  
512 Frey and McClelland, 2009; Moskalenko, 2009; Romanovsky et al., 2010; Vasiliev et al., 2011; Anisimov et al., 2013).  
513 This agrees with large-scale permafrost shifts consisting in southern boundaries moving northward (see Walvoord and  
514 Kurylyk, 2016 for a review). Assuming a “substitution space for time” scenario, and upscaling the data of peat pore  
515 waters obtained in this study, we predict that the shift of the permafrost boundary northward even by 2° latitude will not

516 affect the concentrations of most major and TE in peat pore-waters. The concentrations of DOC, DIC, Ca, Mg, K, Al, Fe,  
517 and trace metals in continuous permafrost zone may remain constant or decrease by a factor of 1.5 to 2 which is often  
518 within the natural variation between different microlandscapes, soil depths and seasons.

519 The ALT is projected to **deepen** more than 30% during this century in the Northern Hemisphere (Anisimov et  
520 al., 2002; Stendel and Christensen, 2002; Dankers et al., 2011). As a general scenario in frozen peatlands of the subarctic,  
521 this increase will bring about the involvement of mineral horizons into water infiltration zone downward the soil profile  
522 (Walvoord and Kurylyk, 2016). The degradation of peat mounds and polygons will be accompanied by the spreading of  
523 hollows and depressions (Pastukhov and Kaverin, 2016). As a result, the water coverage of the watershed will increase  
524 thus enhancing the anaerobic conditions. **On the one hand**, this will increase the fraction of hollows and depressions  
525 containing less concentrated interstitial soil solutions and thus the stock of DOC, major elements and trace metals in soil  
526 fluids will decrease. **On the other hand**, the increasing anaerobic conditions may preferentially mobilize redox sensitive  
527 elements (Fe, Mn, Cr, V...) from the peat to the porewaters. Overall, the share of spring runoff from the mounds to the  
528 rivers and lakes will decrease whereas during the summer baseflow, the input from the hollows and depressions to the  
529 hydrological network will increase.

530 The concept "**substituting** space for time" allows foreseeing the consequences of soil warming in the continuous  
531 permafrost zone of the WSL peatlands on the adjacent river chemistry and export of carbon and metals from the  
532 watersheds. This prediction can be made only for small rivers of the WSL (e.g., watershed area < 10,000 km<sup>2</sup>) which  
533 drain the adjacent peatlands, have no underground feeding and flow essentially during unfrozen period of the year (see  
534 Pokrovsky et al., 2015, 2016a). For this, two basic scenarios can be considered: (i) a constant latitudinal pattern of  
535 permafrost distribution (no boundary migration) but complete disappearance of peat mounds and their replacement by  
536 hollows and depressions and (ii) a shift of the permafrost boundary to the north and transformation of the continuous  
537 permafrost zone into the discontinuous and transformation of the discontinuous permafrost into the sporadic without  
538 changing the microlandscape distribution. **As a first approximation, we assume no change in precipitation,  
539 evapotranspiration and riverine runoff in the northern part of WSL (60-68°N), given that the drying trend will be  
540 pronounced only in the regions located to the south of 60 °N (Alexandrov et al., 2016).**

541 The first scenario yields a decrease in the concentrations of DOC, DIC, major cations and trace metals in  
542 porewaters of continuous permafrost zone by not more than 30%. This estimation stems from the maximal difference in  
543 element concentration between mounds and hollows (Table 2) **and typical proportion of mounds in the terrestrial  
544 landscape of the WSL (35±15 %, Novikov et al., 2009 and authors' unpublished data).** The second scenario is based on  
545 the latitudinal patterns of element concentration in the peat porewaters (Table 3 and Figs 3-5, S4, S5). For this, a linear  
546 dependence of element concentration in all microlandscapes on the latitude given in Figs. 3 to 5 can be used. A two-  
547 degree northward shift in the position of the permafrost boundaries will bring about a factor of 1.3±0.2 decrease in Ca,  
548 Mg, Sr, Al, Fe, Ti, Mn, Ni, Co, V, Zr, Hf, Th, and REEs concentration in continuous and discontinuous permafrost  
549 zones. Note that a possible decrease in DOC, SUVA<sub>280</sub>, Ca, Mg, Fe, Sr will not exceed 20% of their actual values.  
550 Finally, there may be an increase in Cl, Na, K, Rb, Cs, Zn, P and Sb concentration by 30±10%. In both scenarios of  
551 permafrost thawing in the WSL peatlands we do not expect any sizeable increase of soil porewater concentration in DOC  
552 and metal and enhancement of the export of solutes by small-size rivers which are not connected to the underground  
553 reservoirs. This contradicts the dominating paradigm of the increase of DOC, DIC, major cations and metal discharge  
554 from the land to the ocean upon the on-going climate warming in other permafrost regions. **Combining both scenario of  
555 permafrost thaw (northward permafrost boundary shift and extending the hollows over mounds) suggests that over the**

556 first decades, relatively fast permafrost coverage shift will not be accompanied by the change of micro-landscapes and  
557 thus the overall decrease of DOC and metal concentration in peat porewaters will be around 20 to 30%. The average rate  
558 of peat formation in Siberian flat-mound bogs is  $0.24 \text{ mm y}^{-1}$  (Inisheva et al., 2013). Thus, taking into account the climate  
559 warming and accelerated peat growth, after 500 to 1000 years which are necessary to form the new ca. 20-cm peat layer,  
560 the second scenario will take over and thus up to 2-fold cumulative element concentration decrease in soil fluids of  
561 continuous permafrost zone may occur. Assuming a dominant feeding of small rivers by soil porewaters transported  
562 along the permafrost boundary, a slight decrease (i.e., < 30 %) of riverine transport of DOC, DIC, Fe, Al, Ca, Mg from  
563 the northern part of the WSL territory to the Arctic Ocean is anticipated. This decrease will be mostly pronounced for  
564 small rivers such as those of the Arctic coastal zone.

565

## 566 **Conclusions**

567

568 A snapshot of peat soil water chemistry allowed to quantify the distribution of DOC, major and trace element in  
569 peat porewaters at the end of the active period across a sizeable gradient of permafrost. We did not confirm a trend of  
570 diminishing DOC and metal concentration in peat porewaters northward, despite a decrease in mean annual temperature,  
571 vegetation density and the active layer thickness. DOC, DIC and most major and TE did not exhibit any statistically  
572 significant trend of concentration with the latitude. A clear trend of increasing concentrations of Mg, Ca, Al, Ti, V, Ni,  
573 Sr, heavy REE, Zr, Hf and Th marked the increase of the influence of silicate mineral weathering. Concentrations of  
574 DOC,  $\text{SO}_4^{2-}$ , B, V, Cs, Th in pore waters in the peat mounds usually exceeded those in hollows and permafrost  
575 subsidences. The water residence time in peat of various densities and the peat chemical composition were hypothesized  
576 to be the main factors controlling the degree of element leaching from the peat column to the pore fluids. Applying a  
577 “substituting space for time” approach for the climate warming scenario in the WSL, we predict that the northward  
578 migration of permafrost boundary and the replacement of thawing frozen peat mounds and polygons by hollows,  
579 depressions and subsidences will decrease the concentrations of DOC, DIC, major cations and trace metals in porewater  
580 of continuous permafrost zone by a factor of  $1.3 \pm 0.2$ . This in turn will decrease the feeding of small rivers and lakes by  
581 peat soil leachates and the overall export of DOC and metals from the WSL territory to the Arctic Ocean may decrease.  
582 As such, the dominating paradigm of the increase of DOC, DIC, major cation and metal export fluxes upon the on-going  
583 climate warming in boreal and subarctic regions should be revised for the case of frozen peatlands.

584

585

## 586 **Data availability**

587 Full data set of major and trace element concentration in porewaters (< 0.45  $\mu\text{m}$ ) across the latitudinal profile of Western  
588 Siberia Lowland is available at the Research Gate,  
589 [https://www.researchgate.net/publication/313058330\\_Element\\_concentrations\\_in\\_peat\\_soil\\_solutions\\_across\\_the\\_micro-](https://www.researchgate.net/publication/313058330_Element_concentrations_in_peat_soil_solutions_across_the_micro-landscapes_and_permafrost_zones_of_western_Siberia_peatlands)  
590 [-landscapes\\_and\\_permafrost\\_zones\\_of\\_western\\_Siberia\\_peatlands](https://www.researchgate.net/publication/313058330_Element_concentrations_in_peat_soil_solutions_across_the_micro-landscapes_and_permafrost_zones_of_western_Siberia_peatlands)

591

592

## 593 **Acknowledgements**

594 We acknowledge support from RFBR Nos. 16-34-60203 mol\_a\_dk, BIO-GEO-CLIM grant from the Russian Ministry of  
595 Science and Education and Tomsk State University (No 14.B25.31.0001), RFFI grants No 15-29-02599, 17-55-16008,  
596 FCP “Kolmogorov” No 14.587.21.0036, and a partial support from and RSF (RNF) grant No 15-17-10009 “Evolution of  
597 thermokarst ecosystems”.

598

599 **References**

- 600
- 601 Abbott, B. W., Larouche, J. R., Jones Jr., J. B., Bowden, W. B., and Balsler, A. W.: Elevated dissolved organic carbon  
602 biodegradability from thawing and collapsing permafrost, *J. Geophys. Res.-Biogeo.*, 119, 2049–2063, 2014.
- 603 Akerman, H. J., Johansson, M.: Thawing permafrost and thicker active layers in sub-arctic Sweden, *Permafrost*  
604 *Periglacial Process.*, 19, 279–292, 2008.
- 605 Alexandrov, G. A., Brovkin, V. A., and Kleinen, T. : The influence of climate on peatland extent in Western Siberia  
606 since the Last Glacial Maximum, *Sci. Reports*, 6, 24784, doi:10.1038/srep24784, 2016.
- 607 Anisimov, O. A., Shiklomanov, N. I. and Nelson, F. E.: Variability of seasonal thaw depth in permafrost regions: A  
608 stochastic modeling approach, *Ecol. Model.*, 153, 217–227, 2002.
- 609 Anisimov, O., Kokorev, V. and Zhil'tsova, Y.: Temporal and spatial patterns of modern climatic warming: Case study of  
610 Northern Eurasia, *Climat. Change*, 118, 871–883, 2013.
- 611 Beaulieu, E., Godderis, Y., Donnadiou, Y., Labat, D., and Roelandt, C.: High sensitivity of the continental-weathering  
612 carbon dioxide sink to future climate change, *Nat. Clim. Change*, 2, 346–349, 2012.
- 613 Bagard, M. L., Chabaux, F., Pokrovsky, O. S., Prokushkin, A. S., Viers, J., Dupré, B., and Stille, P.: Seasonal variability  
614 of element fluxes in two Central Siberian rivers draining high latitude permafrost dominated areas, *Geochim.*  
615 *Cosmochim. Ac.*, 75, 3335–3357, 2011.
- 616 Bagard, M. L., Schmitt, A. D., Chabaux, F., Pokrovsky, O. S., Viers, J., Stille, P., Labolle, F., and Prokushkin, A. S.:  
617 Biogeochemistry of stable Ca and radiogenic Sr isotopes in larch-covered permafrost-dominated watersheds of  
618 Central Siberia, *Geochim. Cosmochim. Ac.*, 114, 169–187, 2013.
- 619 Batuev, V. I.: Formation of water runoff from mound bogs (case study of Western Siberia), *TSPU Bulletin*, 122(7), 146–  
620 152, 2012.
- 621 Barker, A. J., Douglas, T. A., Jacobson, A. D., McClelland, J. W., Ilgen, A. G., Khosh, M. S., Lehn, G. O., and Trainor,  
622 T. P.: Late season mobilization of trace metals in two small Alaskan arctic watersheds as a proxy for landscape  
623 scale permafrost active layer dynamics, *Chem. Geol.*, 381, 180–193, 2014.
- 624 Beilman, D. W., MacDonald, G. M., Smith, L. C., and Reimer, P. J.: Carbon accumulation in peatlands of West Siberia  
625 over the last 2000 years, *Global Biogeochem. Cy.*, 23(1), GB1012, doi:10.1029/2007GB003112, 2009.
- 626 Botch, M. S., Kobak, K. I., Vinson, T. S., and Kolchugina, T. P.: Carbon pools and accumulation in peatlands of the  
627 former Soviet Union, *Global Biogeochem. Cy.*, 9(1), 37–46, doi:10.1029/94GB03156, 1995.
- 628 Blodau, C. and Moore, T. R.: Experimental response of peatland carbon dynamics to a water table fluctuation, *Aquat.*  
629 *Sci.*, 65–47, doi:10.1007/s000270300004, 2003.
- 630 Bobrik, A. A., Goncharova, O. Yu., Matyshak, G. V., Ryzhova, I. M., Moskalenko, N. G., Ponomareva, O. E., Ogneva,  
631 O. A.: Relationship of active layer thickness and landscape parameters of peatlands in the north of west Siberia  
632 (Nadym station), *Earth's Cryosphere*, XIX(4), 31–38, 2015.
- 633 Brouchkov, A.: Nature and distribution of frozen saline sediments on the Russian Arctic Coast, *Permafrost Periglacial*  
634 *Proc.*, 13, 83–90, 2002.
- 635 Brown, J., Ferrians Jr, O. J., Heginbottom, J. A., and Melnikov, E. S.: Circum-arctic map of permafrost and ground ice  
636 conditions, Boulder, CO 80309-0449 USA, National Snow and Ice Data Center, Digital media, 1998, revised  
637 February 2001.
- 638 Charman, D. J., Beilman, D. W., Blaauw, M., Booth, R. K., Brewer, S., Chambers, F. M., Christen, J. A., Gallego-Sala,  
639 A., Harrison, S. P., Hughes, P. D. M., Jackson, S. T., Korhola, A., Mauquoy, D., Mitchell, F. J. G., Prentice, I.  
640 C., van der Linden, M., De Vleeschouwer, F., Yu, Z. C., Alm, J., Bauer, I. E., Corish, Y. M. C., Garneau, M.,  
641 Hohl, V., Huang, Y., Karofeld, E., Le Roux, G., Loisel, J., Moschen, R., Nichols, J. E., Nieminen, T. M.,  
642 MacDonald, G. M., Phadtare, N. R., Rausch, N., Sillasoo, Ü., Swindles, G. T., Tuittila, E.-S., Ukonmaanaho,  
643 L., Väliranta, M., van Bellen, S., van Geel, B., Vitt, D. H., and Zhao, Y.: Climate-related changes in peatland  
644 carbon accumulation during the last millennium, *Biogeosciences*, 10, 929–944, doi:10.5194/bg-10-929-2013,  
645 2013.
- 646 Clark, J. M., Heinemeyer, A., Martin, P., and Bottrell, S. H.: Processes controlling DOC in pore water during simulated  
647 drought cycles in six different UK peats, *Biogeochemistry*, 109(1–3), 109–253, doi:10.1007/s10533-011-9624-  
648 9, 2012.
- 649 Cory, R. M., Crump, B. C., Dobkowski, J. A., and Kling, G. W.: Surface exposure to sunlight stimulates CO2 release  
650 from permafrost soil carbon in the Arctic, *Proc. Natl. Acad. Sci. USA*, 110, 3429–3434, 2013.
- 651 Dankers, R., Burke, E. J., Price, J.: Simulation of permafrost and seasonal thaw depth in the JULES land surface scheme,  
652 *Cryosphere*, 5(3), 773–790, 2011.
- 653 Dielemann, C. M., Lindo, Z., McLaughlin, J. W., Craig, A. E., Branfireum, B. A.: Climate change effects on peatland  
654 decomposition and porewater dissolved organic carbon biogeochemistry, *Biogeochemistry*, 128, 385–396,  
655 2016.
- 656 Dessert C., Dupré B., Gaillardet J., Francois L., Allegre C.J.: Basalt weathering laws and the impact of basalt weathering  
657 on the global carbon cycle. *Chem. Geol.*, 202, 257–273, 2003.
- 658 Drake, T. W., Wickland, K. P., Spencer, R. G. M., McKnight, D. M., Striegl, R. G.: Ancient low-molecular-weight



- 659 organic acids in permafrost fuel rapid carbon dioxide production upon thaw, *PNAS*, 112(45), 13946–13951,  
660 doi:10.1073/pnas.1511705112, 2015.
- 661 Feng, X. J., Vonk, J. E., van Dongen, B. E., Gustafsson, O., Semiletov, I. P., Dudarev, O. V., Wang, Z. H., Montlucon,  
662 D. B., Wacker, L., and Eglinton, T.I.: Differential mobilization of terrestrial carbon pools in Eurasian Arctic  
663 river basins, *P. Natl. Acad. Sci. USA*, 110, 14168–14173, 2013.
- 664 Fouché, J., Keller, C., Allard, M., Ambrosi, J. P.: Increased CO<sub>2</sub> fluxes under warming tests and soil solution chemistry  
665 in Histic and Turbic Cryosols, Salluit, Nunavik, Canada, *Soil Biol. Biochem.*, 68, 185–199,  
666 doi:10.1016/j.soilbio.2013.10.007, 2014.
- 667 Fraysse, F., Pokrovsky, O.S., Meunier, J-D.: Experimental study of terrestrial plant litter interaction with aqueous  
668 solutions, *Geochim. Cosmochim. Acta*, 74, 70–84, 2010.
- 669 Frey, K. E. and Smith, L. C.: Amplified carbon release from vast West Siberian peatlands by 2100, *Geophys. Res. Lett.*,  
670 32, L09401, doi:10.1029/2004GL022025, 2005.
- 671 Frey, K. E., McClelland, J. W., Holmes, R. M., and Smith, L. C.: Impacts of climate warming and permafrost thaw on the  
672 riverine transport of nitrogen and phosphorus to the Kara Sea, *J. Geophys. Res.*, 112, G04S58,  
673 doi:10.1029/2006JG000369, 2007a.
- 674 Frey, K. E., Siegel, D. I. and Smith, L. C.: Geochemistry of west Siberian streams and their potential response to  
675 permafrost degradation, *Water Resources Res.*, 43, W03406, doi:10.1029/2006WR004902, 2007b.
- 676 Frey, K. E. and Smith, L. C.: How well do we know northern land cover? Comparison of four global vegetation and  
677 wetland products with a new ground-truth database for West Siberia, *Global Biogeochem. Cy.*, 21, GB1016,  
678 doi:10.1029/2006GB002706, 2007.
- 679 Frey, K. E. and McClelland, J. W.: Impacts of permafrost degradation on arctic river biogeochemistry, *Hydrol. Process.*,  
680 23, 169–182, 2009.
- 681 Frey, K. E., Sobczak, W. V., Mann, P. J., and Holmes, R. M.: Optical properties and bioavailability of dissolved organic  
682 matter along a flow-path continuum from soil pore waters to the Kolyma River mainstem, East Siberia,  
683 *Biogeosciences*, 13, 2279–2290, doi:10.5194/bg-13-2279-2016, 2016.
- 684 Gangloff, S., Stille, P., Schmitt, A.-D., Chabaux, F.: Factors controlling the chemical composition of colloidal and  
685 dissolved fractions in soil solutions and the mobility of trace elements in soils, *Geochim. Cosmochim. Acta*,  
686 189, 37–57. doi:10.1016/j.gca.2016.06.009, 2016.
- 687 Geibe, C.E., Danielsson, R., van Hees, P.A.W., Lundström, U.S.: Comparison of soil solution chemistry sampled by  
688 centrifugation, two types of suction lysimeters and zero-tension lysimeters, *Appl. Geochem.*, 21(12), 2096–  
689 2111, doi: 10.1016/j.apgeochem.2006.07.010, 2006.
- 690 Gentsch, N., Mikutta, R., Alves, R. J. E., Barta, J., Capek, P., Gitte, A., Hugelius, G., Kuhry, P., Lashchinskiy, N.,  
691 Palmtag, J., Richter, A., Santrucková, H., Schneckner, J., Shibistova, O., Urich, T., Wild, B., and  
692 Guggenberger, G.: Storage and transformation of organic matter fractions in cryoturbated permafrost soils  
693 across the Siberian Arctic, *Biogeosciences*, 12, 4525–4542. doi:10.5194/bg-12-4525-2015, 2015.
- 694 Giesler, R., Högberg, M. N., Strobel, B. W., Richter, A., Nordgren, A., and Högberg, P.: Production of dissolved organic  
695 carbon and low-molecular weight organic acids in soil solution driven by recent tree photosynthate,  
696 *Biogeochemistry*, 84, 1–12, 2006.
- 697 Giesler, R., Lyon, S. W., Mörth, C.-M., Karlsson, J., Karlsson, E. M., Jantze, E. J., Destouni, G., and Humborg, C.:  
698 Catchment-scale dissolved carbon concentrations and export estimates across six subarctic streams in northern  
699 Sweden, *Biogeosciences*, 11, 525–537, doi:10.5194/bg-11-525-2014, 2014.
- 700 Goldberg, S. D., Knorr, K.-H., Blodau, C., Lischeid, G., Gebauer G.: Impact of altering the water table height of an  
701 acidic fen on N<sub>2</sub>O and NO fluxes and soil concentrations, *Global Change Biol.*, 16(1), 220,  
702 doi:10.1111/j.1365-2486.2009.02015.x, 2010.
- 703 Golovleva, Yu. A., Avetov, N. A., Bruand, A., Kiryushin, A. V., Tolpeshta, I. I., Krasil'nikov, P. V.: Genesis of taiga  
704 poorly differentiated soils in West Siberia, *Lesovedenie*, № 2, 83–93, 2017,  
705 <http://lesovedenie.ru/index.php/forestry/article/view/983> (in Russian).
- 706 Griffiths, N., Sebestyen, S. D.: Dynamic vertical profiles of peat porewater chemistry in a northern peatland, *Wetlands*,  
707 36(6), 1119–1130, 2016.
- 708 Grosse, G., Goetz, S. J., McGuire, A. D., Romanovsky, V. E., Schuur, E. A. G.: Changing permafrost in a warming  
709 world and feedbacks to the Earth system, *Environ. Res. Lett.*, 11(4), 040201, 2016.
- 710 Guo, L., Ping, C. L., and MacDonald, R.W.: Mobilization pathways of organic carbon from permafrost to Arctic rivers in  
711 a changing climate, *Geophys. Res. Lett.*, 34, L13603, doi:10.1029/2007GL030689, 2007.
- 712 Haapalehto, T., Vasander, H., Jauhiainen, S., Tahvanainen, T., Kotiaho, J. S.: The effects of peatland restoration on water  
713 table depth, elemental concentrations, and vegetation: 10 years of changes, *Restor Ecol.*, 19, 587–598, 2011.
- 714 Hendershot, W. H., Savoie, S., Courchesne, F.: Simulation of stream-water chemistry with soil solution and groundwater  
715 flow contributions, *J Hydrol.*, 136(1–4), 237–252, doi:10.1016/0022-1694(92)90013-L, 1992.
- 716 Holmes, R. M., McClelland, J. W., Peterson, B. J., Tank, S. E., Bulygina, E., Eglinton, T. I., Gordeev, V. V., Gurtovaya,  
717 T. Y., Raymond, P. A., Repeta, D. J., Staples, R., Striegl, R. G., Zhulidov, A. V., and Zimov, S. A.: Seasonal

- 718 and annual fluxes of nutrients and organic matter from large rivers to the Arctic Ocean and surrounding seas,  
719 *Estuar. Coast.*, 35, 369–382, doi:10.1007/s12237-011-9386-6, 2012.
- 720 Herndon, E. M., Yang, Z., Bargar, J., Janot, N., Regier, T. Z., Graham, D. E., Wullschleger, S. D., Gu, B., Liang, L.:  
721 Geochemical drivers of organic matter decomposition in arctic tundra soils, *Biogeochemistry*, 126(3), 397–  
722 414, doi:10.1007/s10533-015-0165-5, 2015.
- 723 Holmes, R. M., Coe, M. T., Fiske, G. J., Gurtovaya, T., McClelland, J. W., Shiklomanov, A. I., Spencer, R. G. M., Tank, S.  
724 E., Zhulidov, A. V.: Climate change impacts on the hydrology and biogeochemistry of Arctic Rivers, in: *Climatic  
725 Changes and Global warming of Inland Waters: Impacts and Mitigation for Ecosystems and Societies*, Goldman,  
726 C. R., Kumagi, M., and Robarts, R. D., John Wiley and Sons, Ltd., Publication, The Atrium, Southern Gate,  
727 Chichester, West Sussex, UK, 1–26, 2013.
- 728 Hodgkins, S. B., Tfaily, M. M., McCalley, C. K., Logan, T. A., Crill, P. M., Saleska, S. R., Rich, V. I., Chanton, J. P.:  
729 Changes in peat chemistry associated with permafrost thaw increase greenhouse gas production, *PNAS*,  
730 111(16), 5819–5824, doi:10.1073/pnas.1314641111, 2014.
- 731 Hodgkins, S. B., et al.: Elemental composition and optical properties reveal changes in dissolved organic matter along a  
732 permafrost thaw chronosequence in a subarctic peatland, *Geochim. Cosmochim. Acta*, 187, 123–140, 2016.
- 733 Ilina, S. M., Drozdova, O. Y., Lapitskiy, S. A., Alekhin, Y. V., Demin, V. V., Zavgorodnyay, Y. A., Shirokova, L. S.,  
734 Viers, J., Pokrovsky, O. S.: Size fractionation and optical properties of dissolved organic matter in the  
735 continuum soil solution-bog-river and terminal lake of a boreal watershed, *Organic Geochem.*, 66, 14–24.  
736 doi:10.1016/j.orggeochem.2013.10.008, 2014.
- 737 Inisheva, L. I., Kobak, K. I., Turchinovich, I. E.: Evolution of the paludification process, and carbon accumulation rate in bog  
738 ecosystems of Russia, *Geography Natural Resources*, 34 (3), 246–253, doi:10.1134/S1875372813030086, 2013.
- 739 Ivanov, K. E., Novikov, S. M.: Bogs of western Siberia, their composition and hydrological regime, Leningrad,  
740 Gidrometeoizdat, 448 pp., 1976 (in Russian).
- 741 Jantze, E. J., Lyon, S. W., and Destouni, G.: Subsurface release and transport of dissolved carbon in a discontinuous  
742 permafrost region, *Hydrol. Earth Syst. Sc.*, 17, 3827–3839, doi:10.5194/hess-17-3827-2013, 2013.
- 743 Jessen, S., Holmslykke, H. D., Rasmussen, K., Richardt, N., Holm, P. E.: Hydrology and pore water chemistry in a  
744 permafrost wetland, Ilulissat, Greenland, *Water Resources Res.*, 50(6), 4760–4774,  
745 doi:10.1002/2013WR014376, 2014.
- 746 Jorgenson, M. T., Harden, J., Kanevskiy, M., O'Donnel, J., Wickland, K., Ewing, S., Manies, K., Zhuang, Q., Shur, Y.,  
747 Striegl, R., Koch, J.: Reorganization of vegetation, hydrology and soil carbon after permafrost degradation across  
748 heterogeneous boreal landscapes, *Environ. Res. Lett.*, 8, Art No 035017, doi: 10.1088/1748-9326/8/035017, 2013.
- 749 Kaiser, C., Meyer, H., Biasi, C., Rusalimova, O., Barsukov, P., and Richter, A.: Conservation of soil organic matter through  
750 cryoturbation in arctic soils in Siberia, *J. Geophys. Res.*, 112, 9–17, 2007.
- 751 Karavanova, E. I., Malinina, M. S.: Spatial and temporal variation in the elemental composition of soil solution from  
752 gleyic peaty-podzolic soils, *Eurasian Soil Sci.*, 40(8), 830–838, doi:10.1134/S1064229307080042, 2007.
- 753 Kawahigashi, M., Kaiser, K., Kalbitz, K., Rodionov, A., and Guggenberger, G.: Dissolved organic matter in small streams  
754 along a gradient from discontinuous to continuous permafrost, *Glob. Change Biol.*, 10, 1576–1586,  
755 doi:10.1111/j.1365-2486.2004.00827.x, 2004.
- 756 Keller, K., Blum, J. D. and Kling, G. W.: Stream geochemistry as an indicator of increasing permafrost thaw depth in an  
757 Arctic watershed, *Chem. Geol.*, 273, 76–81, 2010.
- 758 Koch, J. C., Runkel, R. L., Striegl, R., McKnight, D. M.: Hydrologic controls on the transport and cycling of carbon and  
759 nitrogen in a boreal catchment underlain by continuous permafrost, *J. Geophys. Res. – Biogeosciences*,  
760 118(2), 698–712, doi:10.1002/jgrg.20058, 2013.
- 761 Köhler, S. J., Lidman, F. and Laudon, H.: Landscape types and pH control organic matter mediated mobilization of Al,  
762 Fe, U and La in boreal catchments, *Geochim. Cosmochim. Acta*, 135, 190–202, 2014.
- 763 Kokelj, S. V., Jenkins, R. E., Milburn, D., Burn, C. R., Snow, N.: The influence of thermokarst disturbance on the water  
764 quality of small upland lakes, Mackenzie Delta Region, Northwest Territories, Canada, *Permafrost Periglacial  
765 Res.*, 16, 343–353, doi:10.1002/ppp.536, 2005.
- 766 Kokelj, S. V., Zajdlík, B., Thompson, M. S.: The impacts of thawing permafrost on the chemistry of lakes across the  
767 subarctic boreal-tundra transition, Mackenzie Delta region, Canada. *Permafrost Periglacial Res.*, 20(2), 185–  
768 199, doi:10.1002/ppp.641, 2009.
- 769 Kremenetski, K. V., Velichko, A. A., Borisova, O. K., MacDonald, G. M., Smith, L. C., Frey, K. E., and Orlova, L. A.:  
770 Peatlands of the West Siberian Lowlands: Current knowledge on zonation, carbon content, and Late  
771 Quaternary history, *Quaternary Sci. Rev.*, 22, 703–723, 2003.
- 772 Laurion, I., Vincent, W.F., MacIntyre, S., Retamal, L., Dupont, C., Francus, P., Pienitz, R.: Variability in greenhouse gas  
773 emissions from permafrost thaw ponds, *Limnol. Oceanogr.*, 55, 115–133, 2010.
- 774 Leach, J. A., Larsson, A., Wallin, M. B., Nilsson, M. B., and Laudon, H.: Twelve year interannual and seasonal  
775 variability of stream carbon export from a boreal peatland catchment, *J. Geophys. Res. Biogeosci.*, 121, 1851–  
776 1866, doi:10.1002/2016JG003357, 2016.

- 777 Liu, L., Chen, H., Zhu, Q., Yang, G., Zhu, E., Hu, J., Peng, C., Jiang, L., Zhan, W., Ma, T., He, Y., Zhu, D.: Responses  
778 of peat carbon at different depths to simulated warming and oxidizing, *Sci. Total Environ.*, 548–549, 429–440.  
779 doi:10.1016/j.scitotenv.2015.11.149, 2016.
- 780 Lobbes, J. M., Fitznar, H. P., and Kattner, G.: Biogeochemical characteristics of dissolved and particulate organic matter  
781 in Russian rivers entering the Arctic Ocean, *Geochim. Cosmochim. Ac.*, 64, 2973–2983, 2000.
- 782 Lupachev, A. V., Gubin, S. V., Veremeeva, A. A., Kaverin, D. A., Pastukhov, A. V., Yakimov, A. S.: Microrelief of the  
783 permafrost table: structure and ecological functions, *Earth's Cryosphere*, XX(2), 3–14, 2016.
- 784 MacLean, R., Oswood, M. W., Irons, J. G. III, McDowell, W. H.: The effect of permafrost on stream biogeochemistry:  
785 A case study of two streams in the Alaskan (USA) taiga, *Biogeochemistry*, 47, 239–267, 1999.
- 786 Makhatkov, I. D., Ermolov, Yu. V.: The thermal regime of active layer of pit-covered terrain in northern taiga,  
787 *Mezhdunarodnyi Zhurnal Prikladnukh i Fundamentalnukh Issledovaniy (Internat. J. Appl. Fund. Studies)*,  
788 215(11), 400–407, 2015.
- 789 Manasyrov, R. M., Pokrovsky, O. S., Kirpotin, S. N. and Shirokova, L. S.: Thermokarst lake waters across the  
790 permafrost zones of western Siberia, *Cryosphere*, 8, 1177–1193, 2014.
- 791 Manasyrov, R. M., Vorobyev, S. N., Loiko, S. V., Kritzkov, I. V., Shirokova, L. S., Shevchenko, V. P., Kirpotin, S. N.,  
792 Kulizhsky, S. P., Kolesnichenko, L. G., Zemtsov, V. A., Sinkinov, V. V. and Pokrovsky, O. S.: Seasonal  
793 dynamics of organic carbon and metals in thermokarst lakes from the discontinuous permafrost zone of  
794 western Siberia, *Biogeosciences*, 12, 3009–3028, 2015.
- 795 **Manasyrov, R. M., Shirokova, L. S. and Pokrovsky O. S.: Experimental modeling of thaw lake water evolution in  
796 discontinuous permafrost zone: role of peat and lichen leaching and ground fire, *Sci. Tot. Environ.*, 580, 245-  
797 257, 2017.**
- 798 Mann, P. J., Davydova, A., Zimov, N., Spencer, R. G. M., Davydov, S., Bulygina, E., Zimov, S., and Holmes, R. M.:  
799 Controls on the composition and lability of dissolved organic matter in Siberia's Kolyma River basin, *J.*  
800 *Geophys. Res.-Biogeo.*, 117, G01028, doi:10.1029/2011JG001798, 2012.
- 801 Mann, P. J., Eglinton, T. I., McIntyre, C. P., Zimov, N., Davydova, A., Vonk, J. E., Holmes, R. M., Spencer, R. G. M.:  
802 Utilization of ancient permafrost carbon in headwaters of Arctic fluvial networks, *Nat Commun.*, 6,  
803 doi:10.1038/ncomms8856, 2015.
- 804 Marlin, C., Dever, L., Vachier, P., Courty, M. A.: Chemical and isotopic changes in soil-water during permafrosting of an  
805 active layer on continuous permafrost (Brogger-Peninsula, Svalbard), *Canad. J. Earth Sci.*, 30(4), 806–813,  
806 1993.
- 807 Mavromatis, V., Prokushkin, A. S., Pokrovsky, O. S., Viers, J., and Korets, M. A.: Magnesium isotopes in permafrost-  
808 dominated Central Siberian larch forest watersheds, *Geochim. Cosmochim. Ac.*, 147, 76–89, 2014.
- 809 Michalzik, B., Kalbitz, K., Park, J.-H., Solinger, S. and Matzner, E.: Fluxes and concentrations of dissolved organic  
810 carbon and nitrogen - A synthesis for temperate forests, *Biogeochemistry*, 52, 173–205, 2001.
- 811 Morison, M.Q., Macrae, M. L., Petrone, R. M., Fishback, L.: Seasonal dynamics in shallow freshwater pond-peatland  
812 hydrochemical interactions in a subarctic permafrost environment, *Hydrol. Proc.*, 31(2), 462–475, 2017.
- 813 Moskalenko, N. G.: Permafrost and vegetation changes in the Nadym region of West Siberian northern taiga due to the  
814 climate change and technogenesis, *Kriosfera Zemli*, 8(4), 18–23, 2009.
- 815 **Moulton, K. L., West, J., Berner, R. A.: Solute flux and mineral mass balance approaches to the quantification of plant  
816 effects on silicate weathering, *Am. J. Sci.*, 300, 539-570, 2000.**
- 817 Muller, F. L. L., Chang, K.-C., Lee, C.-L. and Chapman, S. J.: Effects of temperature, rainfall and conifer felling  
818 practices on the surface water chemistry of northern peatlands, *Biogeochemistry*, 126, 343–362, 2015.
- 819 **Natali, S. M., Schuur, E. A. G., Trucco, C., Pries, C. E. H., Crummer, K. G., and Lopez, A. F. B.: Effects of experimental  
820 warming of air, soil and permafrost on carbon balance in Alaskan tundra, *Global Change Biol.*, 17(3), 1394-  
821 1407, DOI: 10.1111/j.1365-2486.2010.02303.x, 2011.**
- 822 **Natali, S. M., Schuur, E. A. G., Mauritz, M., Schade, J. D., Celis, G., Crummer, K. G., Johnston, C., Krapek, J.,  
823 Pegoraro, E., Salmon, V. G., Webb, E. E., Permafrost thaw and soil moisture driving CO<sub>2</sub> and CH<sub>4</sub> release  
824 from upland tundra, *J. Geophys. Res. – Biogeosciences*, 120(3), 525-537, DOI: 10.1002/2014JG002872, 2015.**
- 825 **Neubauer, E., Kohler, S.J., von der Kammer, F., Laudon, H., and Hofmann, T.: Effect of pH and stream order on iron and  
826 arsenic speciation in boreal catchments, *Environ. Sci. Technol.*, 47, 7120-7128, 2013.**
- 827 Novikov, S. M., Moskvina, Y. P., Trofimov, S. A., Usova, L. I., Batuev, V. I., Tumanovskaya, S. M., Smirnova, V. P.,  
828 Markov, M. L., Korotkevich, A. E., and Potapova, T. M.: Hydrology of bog territories of the permafrost zone  
829 of western Siberia, *BBM publ. House, St. Petersburg*, 535 pp., 2009 (in Russian).
- 830 **Olefeldt, D., and Roulet, N. T.: Effects of permafrost and hydrology on the composition and transport of dissolved  
831 organic carbon in a subarctic peatland complex, *J. Geophys. Res.*, 117, G01005, doi:10.1029/2011JG001819,  
832 2012.**
- 833 **Olefeldt, D., Roulet, N. T., Giesler, R., and Persson, A.: Total waterborne carbon export and DOC composition from ten  
834 nested subarctic peatland catchments – importance of peatland cover, groundwater influence, and inter-annual  
835 variability of precipitation patterns, *Hydrol. Process.*, 27, 2280–2294, 2013.**

- 836 Olefeldt, D., Persson, A., and Turetsky, M. R.: Influence of the permafrost boundary on dissolved organic matter  
837 characteristics in rivers within the Boreal and Taiga plains of western Canada, *Environ. Res. Lett.*, 9, Art No  
838 035005, doi:10.1088/1748-9326/9/3/035005, 2014.
- 839 Ovchinnikov, S. M., Sokolova, T. A., and Targulian, V. P.: Clay minerals of clay loam soils of tundra and forest-tundra  
840 of western Siberia, *Pochvovedenie (Soil Science)*, 12, 90–103, 1973.
- 841 Panova N. K., Antipina T. G., Gilev A.V., Trofimova S. S., Zinoviev E.V., and Erokhin N. G. Holocene dynamics of  
842 vegetation and ecological conditions in the Southern Yamal Peninsula according to the results of  
843 comprehensive analysis of a relict peat bog deposit, *Russ. J. Ecol.*, 41(1), 20–27, DOI:  
844 10.1134/S1067413610010042, 2010.
- 845 Pastukhov, A. V., Marchenko-Vagapova, T. I., Kaverin, D. A., and Goncharova, N. N.: Genesis and evolution of peat  
846 plateaus in the sporadic permafrost area in the European North-East (middle basin of the Kosyu river), *Earth's  
847 Cryosphere*, XX(1), 3–13, [http://www.izdatgeo.ru/pdf/earth\\_cryo/2016-1/3\\_eng.pdf](http://www.izdatgeo.ru/pdf/earth_cryo/2016-1/3_eng.pdf), 2016.
- 848 Pastukhov, A. V. and Kaverin, D. A.: Ecological state of peat plateaus in northeastern European Russia, *Russ. J. Ecol.*,  
849 47(2), 125–132, doi:10.1134/S1067413616010100, 2016.
- 850 Pavlov, A. V. and Moskalenko, N. G.: The thermal regime of soils in the north of Western Siberia, *Permafrost Periglac.  
851 Proc.*, 13, 43–51, doi:10.1002/ppp.409, 2002.
- 852 Pokrovsky, O. S., Schott, J., and Dupre, B.: Trace element fractionation and transport in boreal rivers and soil porewaters of  
853 permafrost-dominated basaltic terrain in Central Siberia, *Geochim. Cosmochim. Ac.*, 70, 3239–3260, 2006.
- 854 Pokrovsky, O. S., Shirokova, L. S., Kirpotin, S. N., Audry, S., Viers, J., and Dupré, B.: Effect of permafrost thawing on the  
855 organic carbon and metal speciation in thermokarst lakes of western Siberia, *Biogeosciences*, 8, 565–583, 2011.
- 856 Pokrovsky, O. S., Reynolds, B. C., Prokushkin, A. S., Schott, J., and Viers, J.: Silicon isotope variations in Central Siberian  
857 rivers during basalt weathering in permafrost-dominated larch forests, *Chem. Geol.*, 355, 103–116, 2013.
- 858 Pokrovsky, O. S., Manasypov, R. M., Shirokova, L. S., Loiko, S. V., Krickov, I. V., Kopysov, S. G., et al.: Permafrost  
859 coverage, watershed area and season control of dissolved carbon and major elements in western Siberia rivers,  
860 *Biogeosciences*, 12, 6301–6320, 2015.
- 861 Pokrovsky, O. S., Manasypov, R. M., Loiko, S. V., Krickov, I. A., Kopysov, S. G., Kolesnichenko, L., G., Vorobyev, S.  
862 N., Kirpotin, S. N.: Trace element transport in western Siberia rivers across a permafrost gradient,  
863 *Biogeosciences*, 13, 1877–1900, 2016a.
- 864 Pokrovsky, O. S., Manasypov, R. M., Loiko, S. V., Shirokova, L. S.: Organic and organo-mineral colloids of  
865 discontinuous permafrost zone, *Geochim. Cosmochim. Ac.*, 188, 1–20, 2016b.
- 866 Polishchuk, Y. M., Bogdanov, A. N., Polishchuk, V. Y., Manasypov, R. M., Shirokova, L. S., Kirpotin, S. N., Pokrovsky,  
867 O. S.: Size-distribution, surface coverage, water, carbon and metal storage of thermokarst lakes (> 0.5 ha) in  
868 permafrost zone of the Western Siberia Lowland, *Water*, submitted, 2016.
- 869 Ponomareva, O. E., Gravis, A. G., and Berdnikov, N. M.: Contemporary dynamics of frost mounds and flat peatlands in  
870 north taiga of West Siberia (on the example of Nadym site), *Kriosfera Zemli*, XVI, № 4, 21–30, 2012.
- 871 Pries, C. E. H., Schuur, E. A. G., Natali, S. M., Crummer, K. G.: Old soil carbon losses increase with ecosystem  
872 respiration in experimentally thawed tundra, *Nature Clim. Change*, 6(2), 214, DOI: 10.1038/NCLIMATE2830,  
873 2016.
- 874 Prokushkin, A. S., Kajimoto, T., Prokushkin, S. G., McDowell, W. H., Abaimov, A. P., Matsura, Y.: Climatic factors  
875 influencing fluxes of dissolved organic carbon from the forest floor in a continuous-permafrost Siberian  
876 watershed, *Can. J. For. Res.*, 35, 2130–2140, doi:10.1139/X05-150, 2005.
- 877 Prokushkin, A. S., Pokrovsky, O. S., Shirokova, L. S., Korets, M. A., Viers, J., Prokushkin, S. G., Amon, R.,  
878 Guggenberger, G., and McDowell, W. H.: Sources and export fluxes of dissolved carbon in rivers draining  
879 larch-dominated basins of the Central Siberian Plateau, *Environ. Res. Lett.*, 6, 045212, 14 pp.,  
880 doi:10.1088/1748-9326/6/4/045212, 2011.
- 881 Quinton, W. L., Gray, D. M., Marsh, P.: Subsurface drainage from hummock-covered hillslope in the Arctic tundra, *J.  
882 Hydrol.* 237, 113–125, 2000.
- 883 Quinton, W. L., Pomeroy, J. W.: Transformations of runoff chemistry in the Arctic tundra, Northwest Territories,  
884 Canada, *Hydrological Processes*, 20(14), 2901–2919, doi: 10.1002/hyp.6083, 2006.
- 885 Quinton, W. L., Elliot, T., Price, J. S., Rezanezhad, F., Heck, R.: Measuring physical and hydraulic properties of peat  
886 from X-ray tomography, *Geoderma* 153, 269–277, 2009.
- 887 Quinton, W. L., Baltzer, J. L. : The active-layer hydrology of a peat plateau with thawing permafrost (Scotty Creek,  
888 Canada), *Hydrogeol. J.*, 21(1), 201–220, 2013.
- 889 Raudina, T.V., Loyko, S.V., Krickov, I.V., and Lim, A.G.: Comparing the composition of soil waters of West Siberian  
890 frozen mires sampled by different methods, *Vestnik Tomskogo gosudarstvennogo universiteta. Biologiya –  
891 Tomsk State University Journal of Biology*, 3(35), 26–42. doi: 10.17223/19988591/35/2, 2016.
- 892 Rember, R. D., Trefry, J. H.: Increased concentrations of dissolved trace metals and organic carbon during snowmelt in  
893 rivers of the Alaskan Arctic, *Geochim. Cosmochim. Ac.*, 68(3), 477–489, 2004.
- 894 Reynolds, B., Stevens, P. A., Hughes, S., Brittain, S. A.: Comparison of field techniques for sampling soil solution in an  
895 upland peatland, *Soil Use and Management*, 20(4), 454–456, doi:10.1079/SUM2004277, 2004.

- 896 Rezanezhad, F., Quinton, W. L., Price, J. S., Elrick, D., Elliot, T., Heck, R.: Examining the effect of pore size distribution  
897 and shape on flow through unsaturated peat using computed tomography, *Hydrol. Earth Syst. Sci.* 13, 1993–  
898 2002, 2009.
- 899 Rezanezhad, F., Quinton, W. L., Price, J. S., Elrick, D., Elliot, T., and Shook, K. R.: Influence of pore size and geometry  
900 on peat unsaturated hydraulic conductivity computed from 3D computed tomography image analysis, *Hydrol.*  
901 *Process.* 24, 2983–2994, 2010.
- 902 Rezanezhad F., Price, J.S., Quinton, W.L., Lennartz B., Milojevic, T., Van Cappellen, P.: Structure of peat soils and  
903 implications for water storage, flow and solute transport: A review update for geochemists, *Chem. Geol.*, 429,  
904 75–84, 2016.
- 905 Romanovsky, V. E., Drozdov, D. S., Oberman, N. G., Malkova, G. V., Kholodov, A. L., Marchenko, S. S., Moskalenko,  
906 N. G., Sergeev, D. O., Ukraintseva, N. G., Abramov, A. A., Gilichinsky, D. A., and Vasiliev, A. A.: Thermal  
907 State of Permafrost in Russia, *Permafrost Periglacial Proc.*, 21, 136–155, 2010.
- 908 Schlotter, D., Schack-Kirchner, H., Hildebrand, E.E., von Wilpert, K.: Equivalence or complementarity of soil-solution  
909 extraction methods, *J. Plant Nutr. Soil Sci.*, 175(2), 236–244, doi: 10.1002/jpln.201000399, 2012.
- 910 Schott, J., Pokrovsky, O. S., Oelkers, E. H.: The link between mineral dissolution/precipitation kinetics and solution  
911 chemistry, *Rev. Mineral. Geochem., Thermodynamics and Kinetics of Water-Rock Interaction*, 70, 207–258,  
912 2009.
- 913 Schuur, E. A. G., McGuire, A. D., Schädel, C., Grosse, G., Harden, J. W., Hayes, D.J., Hugelius, G., Koven, C. D., Kuhry, P.,  
914 Lawrence, D. M., Natali, S. M., Olefeldt, D., Romanovsky, V. E., Schaefer, K., Turetsky, M. R., Treat, C. C. and  
915 Vonk, J. E.: Climate change and the permafrost carbon feedback, *Nature*, 520, 171–179. doi:10.1038/nature14338,  
916 2015.
- 917 Shevchenko, V. P., Pokrovsky, O. S., Vorobyev, S. N., Krickov, I. V., Manasypov, R. M., Politova, N. V., Kopysov, S.  
918 G., Dara, O. M., Auda, Y., Shirokova, L. S., Kolesnichenko, L. G., Zemtsov, V. A., and Kirpotin, S. N.:  
919 Impact of snow deposition on major and trace element concentrations and fluxes in surface waters of Western  
920 Siberian Lowland, *Hydrol. Earth Syst. Sci. Discuss.*, doi:10.5194/hess-2016–578, in review, 2016.
- 921 Shirokova, L. S., Pokrovsky, O. S., Kirpotin, S. N., Desmukh, C., Pokrovsky, B. G., Audry, S., and Viers, J.:  
922 Biogeochemistry of organic carbon, CO<sub>2</sub>, CH<sub>4</sub>, and trace elements in thermokarst water bodies in  
923 discontinuous permafrost zones of Western Siberia, *Biogeochemistry*, 113, 573–593, 2013.
- 924 Shotykh, W., Bicalho, B., Cuss, C. W., Duke, M. J. M., Noernberg, T., Pelletier, R., Steinnes, E., and Zaccone, C.: Dust is  
925 the dominant source of “heavy metals” to peat moss (*Sphagnum fuscum*) in the bogs of the Athabasca  
926 Bituminous Sands region on northern Alberta, *Environ. Internat.*, 92–93, 494–506, 2016.
- 927 Shotykh, W., Rausch, N., Nieminen, T. M., Ukonmaanaho, L. and Krachler, M.: Isotopic composition of Pb in peat and  
928 porewaters from three contrasting ombrotrophic bogs in Finland: Evidence of chemical diagenesis in response  
929 to acidification, *Environ. Sci. Technol.*, 50, 9943–9951, 2016.
- 930 Smith, L. C., Macdonald, G. M., Velichko, A. A., Beilman, D. W., Borisova, O. K., Frey, K. E., Kremenetsky, K. V., and  
931 Sheng, Y.: Siberian peatlands as a net carbon sink and global methane source since the early Holocene, *Science*,  
932 303, 353–356, 2004.
- 933 Smith, L. C., Beilman, D. W., Kremenetski, K. V., Sheng, Y., MacDonald, G. M., Lammers, R. B., Shiklomanov, A. I.,  
934 and Lapshina, E. D.: Influence of permafrost on water storage in West Siberian peatlands revealed from a new  
935 database of soil properties, *Permafrost Periglacial Proc.*, 23, 69–79, 2012.
- 936 Smolyakov, B. S.: The problem of acid fallouts in the north of West Siberia, *Sibirskiy Ekologicheskiy Zhurnal*, 1, 21–30,  
937 2000.
- 938 Spencer, R. G. M., Mann, P. J., Dittmar, T., Eglinton, T. I., McIntyre, C., Holmes, R. M., Zimov, N., Stubbins, A.:  
939 Detecting the signature of permafrost thaw in Arctic rivers, *Geophys. Res. Lett.*, 42, 2830–2835,  
940 doi:10.1002/2015GL063498, 2015.
- 941 Spencer, R. G. M., Aiken, G. R., Wickland, K. P., Striegl, R. G., and Hernes, P. J.: Seasonal and spatial variability in  
942 dissolved organic matter quantity and composition from the Yukon River basin, Alaska, *Global Biogeochem.*  
943 *Cy.*, 22, GB4002, doi:10.1029/2008GB003231, 2008.
- 944 Starr, M. and Ukonmaanaho, L.: Levels and Characteristics of TOC in Throughfall, Forest Floor Leachate and Soil  
945 Solution in Undisturbed Boreal Forest Ecosystems, in: *Biogeochemical Investigations of Terrestrial,*  
946 *Freshwater, and Wetland Ecosystems across the Globe, Water, Air, and Soil Pollution, Kluwer Academic*  
947 *Publisher*, 715–729, 2004.
- 948 Stendel, M., Christensen, J. H.: Impact of global warming on permafrost conditions in a coupled GCM, *Geophys. Res.*  
949 *Lett.*, 29(13), Art No 1632, doi:10.1029/2001GL014345, 2002.
- 950 Stepanova, V. M., Pokrovsky, O. S., Viers, J., Mironycheva-Tokareva, N. P., Kosykh, N. P., and Vishnyakova, E. K.:  
951 Major and trace elements in peat profiles in Western Siberia: impact of the landscape context, latitude and  
952 permafrost coverage, *Appl. Geochem.*, 53, 53–70, 2015.
- 953 Striegl, R. G., Aiken, G. R., Dornblaser, M. M., Raymond, P. A., and Wickland, K. P.: A decrease in discharge-  
954 normalized DOC export by the Yukon River during summer through autumn, *Geophys. Res. Lett.*, 32,  
955 L21413, doi:10.1029/2005GL024413, 2005.

- 956 Strack, M., Waddington, J. M., Bourbonniere, R. A., Buckton, E. L., Shaw, K., Whittington, P., Price, J. S.: Effect of  
 957 water table drawdown on peatland dissolved organic carbon export and dynamics, *Hydrol. Proces.*, 22(17),  
 958 3373–3385, doi:10.1002/hyp.6931, 2008.
- 959 Stutter, M. I., Billett, M. F.: Biogeochemical controls on streamwater and soil solution chemistry in a High Arctic  
 960 environment, *Geoderma*, 113(1–2), 127–146, doi:10.1016/S0016-7061(02)00335-X, 2003.
- 961 Syso, A. I.: Features of distribution of chemical elements in soil-forming rocks and soils of Western Siberia, Novosibirsk,  
 962 *Izd-vo SO RAN*, 277 pp, 2007.
- 963 Swindles, G. T., Morris, P. J., Mullan, D., Watson, E. J., Turner, T. E., Roland, T. P. et al.: The long-term fate of  
 964 permafrost peatlands under rapid climate warming, *Scientific Reports* 5, 17951, doi:10.1038/srep17951, 2015.
- 965 Tank, S. E., Lesack, L. F. W., and Hesslein, R. H.: Northern delta lakes as summertime CO<sub>2</sub> absorbers within the Arctic  
 966 landscape, *Ecosystems*, 12, 144–157, 2009.
- 967 Tank, S. E., Frey, K. E., Striegl, R. G., Raymond, P. A., Holmes, R. M., McClelland, J. W., and Peterson, B. J.:  
 968 Landscape level controls on dissolved carbon flux from diverse catchments of the circumboreal, *Glob.*  
 969 *Biogeochem. Cy.*, 26, GB0E02, doi:10.1029/2012GB004299, 2012a.
- 970 Tank, S. E., Raymond, P. A., Striegl, R. G., McClelland, J. W., Holmes, R. M., Fiske, G. J., and Peterson, B. J.: A land-  
 971 to-ocean perspective on the magnitude, source and implication of DIC flux from major Arctic rivers to the  
 972 Arctic Ocean, *Global Biogeochem. Cy.*, 26, GB4018, doi:10.1029/2011GB004192, 2012b.
- 973 Tank, S. E., Striegl, R. G., McClelland, J. W., Kokelj, S. V.: Multi-decadal increases in dissolved organic carbon and  
 974 alkalinity flux from the Mackenzie drainage basin to the Arctic Ocean, *Environ. Res. Lett.*, 11(5), 054015.  
 975 doi:10.1088/1748-9326/11/5/054015, 2016.
- 976 Tarnocai, C., Canadell, J. G., E. Schuur A. G., Kuhry P., Mazhitova G., and Zimov S.: Soil organic carbon pools in the  
 977 northern circumpolar permafrost region, *Global Biogeochem. Cycles*, 23, GB2023,  
 978 doi:10.1029/2008GB003327, 2009.
- 979 Tyrtikov, A. P.: Thawing of soils in tundra of western Siberia, in: *Natural environment of western Siberia*, Issue 3, *Izd-vo*  
 980 *MG*, Moscow, 160–169, 1973 (in Russian).
- 981 Uyguner, C. and Bekbolet, M.: Implementation of spectroscopic parameters for practical monitoring of natural organic  
 982 matter. *Desalination* 176, 47–55, 2005.
- 983 Van Hees, P. A. W., Lundström, U. S. and Giesler, R.: Low molecular weight organic acids and their Al-complexes in  
 984 soil solution-compostion, distribution and seasonal variation in three podzolized soils, *Geoderma* 94, 173–  
 985 200, 2000a.
- 986 Van Hees, P. A. W., Lundström, U. S., Starr, M. and Giesler, R.: Factors influencing aluminium concentrations in soil  
 987 solution from podzols, *Geoderma* 94, 289–310, 2000b.
- 988 Vasyukova, E.V., Pokrovsky, O.S., Viers, J., Oliva, P., Dupré, B., Martin, F., and Candadaup, F.: Trace elements in  
 989 organic- and iron-rich surficial fluids of the boreal zone: Assessing colloidal forms via dialysis and  
 990 ultrafiltration, *Geochim. Cosmochim. Acta*, 74, 449-468, 2010.
- 991 Vasiliev, A. A., Streletskaia, I. D., Shirokov, R. S., and Oblogov, G. E.: Evolution of cryolithozone of coastal zone of  
 992 western Yamal during climate change, *Kriosfera Zemli*, 2, 56–64, 2011 (in Russian).
- 993 Vonk, J. E., Tank, S. E., Mann, P. J., Spencer, R. G. M., Treat, C. C., Striegl, R. G., Abbott, B. W., and Wickland, K. P.:  
 994 Biodegradability of dissolved organic carbon in permafrost soils and aquatic systems: a meta-analysis,  
 995 *Biogeosciences*, 12, 6915–6930, doi:10.5194/bg-12-6915-2015, 2015a.
- 996 Vonk, J. E., Tank, S. E., Bowden, W. B., Laurion, I., Vincent, W. F., Alekseychik, P., Amyot, M., Billet, M. F., Canário,  
 997 J., Cory, R. M., Deshpande, B. N., Helbig, M., Jammet, M., Karlsson, J., Larouche, J., MacMillan, G., Rautio,  
 998 M., Walter Anthony, K. M., Wickland, K. P.: Reviews and syntheses: Effects of permafrost thaw on Arctic  
 999 aquatic ecosystems, *Biogeosciences*, 12, 7129–7167, doi:10.5194/bg-12-7129-2015, 2015b.
- 1000 Walvoord, M. A. and Kurylyk, B. L.: Hydrological impacts of thawing permafrost – a review, *Vadoze Zone J.*, 15(6),  
 1001 doi: 10.2136/vzj2016.01.0010, 2016.
- 1002 Ward, C. P. and Cory, R. M.: Chemical composition of dissolved organic matter draining permafrost soils, *Geochim.*  
 1003 *Cosmochim. Ac.*, 167, 63–79, doi:10.1016/j.gca.2015.07.001, 2015.
- 1004 Weishaar, J. L., Aiken, G. R., Bergamaschi, B. A., Fram, M. S., Fujii, R., and Mopper, K. (2003) Evaluation of specific  
 1005 ultraviolet absorbance as an indicator of the chemical composition and reactivity of dissolved organic carbon,  
 1006 *Env. Sci. Technol.*, 37, 4702–4708, 2003.
- 1007 Wickland, K. P., Aiken, G. R., Butler, K., Dornblaser, M. M., Spencer, R. G. M., and Striegl, R. G.: Biodegradability of  
 1008 dissolved organic carbon in the Yukon River and its tributaries: Seasonality and importance of inorganic  
 1009 nitrogen, *Global Biogeochem. Cycles*, 26, GB0E03, doi:10.1029/2012GB004342, 2012.
- 1010 Working Group WRB: World Reference Base for Soil Resources 2014, International soil classification system for  
 1011 naming soils and creating legends for soil maps, *World Soil Resources Reports*, 106, FAO, Rome, 2014.
- 1012 Yang, Z., Wullschleger, S. D., Liang, L., Graham, D. E., Gu, B.: Effects of warming on the degradation and production  
 1013 of low-molecular-weight labile organic carbon in an Arctic tundra soil, *Soil Biol. Biochem.*, 95, 202–211,  
 1014 doi:10.1016/j.soilbio.2015.12.022, 2016.

1015 Yang, D., Ye, B., and Shiklomanov, A.: Discharge characteristics and changes over the Ob River watershed in Siberia, *J.*  
1016 *Hydrometeorol.*, 5, 595–610, 2004.

1017 Yeghicheyan, D., Bossy, C., Bouhnik Le Coz, M., Douchet, Ch., Granier, G., Heimburger, A., Lacan, F., Lanzanova, A.,  
1018 Rousseau, T. C. C., Seidel, J.-L., Tharaud, M., Candaudap, F., Chmeleff, J., Cloquet, C., Delpoux, S., Labatut,  
1019 M., Losno, R., Pradoux, C., Sivry, Y., and Sonke, J. E.: A Compilation of Silicon, Rare Earth Element and  
1020 Twenty-One other Trace Element Concentrations in the Natural River Water Reference Material SLRS-5  
1021 (NRC-CNRC), *Geostand. Geoanal. Res.*, 37, 449–467, doi:10.1111/j.1751-908X.2013.00232.x, 2013.

1022 Zhang, T. J., Frauenfeld, O. W., Serreze, M. C., Etringer, A., Oelke, C., McCreight, J., Barry, R. G., Gilichinsky, D.,  
1023 Yang, D. Q., Ye, H. C., Ling, F. and Chudinova, S.: Spatial and temporal variability in active layer thickness  
1024 over the Russian Arctic drainage basin, *J. Geophys. Res.-Atmospheres*, 110, doi:10.1029/2004JD005642,  
1025 2005.

Table 1. Physico-geographical, permafrost and soil parameters of 5 study sites.

Site	Latitude, °N	MAT, °C	Mean annual precipitation, mm	Mineral substrate	Micro-landscapes	Peat thickness, m	Seasonal thaw depth, cm	Soil type (WRB, 2014)
Tazovsky, (Tz)	67.4	−9.1°C	363	Clay loam and loam	polygon	2.0–4.0	41	Dystric Hemic Epicryic Histosols (Hyperorganic); Dystric Murshic Hemic Epicryic Histosols (Hyperorganic)
					permafrost subsidences		55	Dystric Epifibric Hemic Cryic Histosols (Hyperorganic)
					frost crack		44	Dystric Epifibric Cryic Histosols (Hyperorganic)
					hollows	0.2–1.5	65	Dystric Fibric Cryic Histosols; Histic Reductaquic Cryosols (Clayic)
Urengoy, (Ur)	66.1	−7.8°C	453	Loam and silt loam	peat mounds	2.0–2.5	49	Dystric Hemic Epicryic Histosols (Hyperorganic)
					hollows	0.3–1.2	98	Histic Reductaquic Cryosols (Loamic); Dystric Fibric Histosols (Gelic)
Pangody, (Pg)	65.9	−6.4°C	484	Loam	peat mounds	0.2–1.3	49	Dystric Hemic Epicryic Histosols; Histic Cryosols (Loamic); Histic Oxyaquic Turbic Cryosols (Loamic)
					permafrost subsidences	0.6–1.1	74	Dystric Hemic Endocryic Histosols
					hollows	0.3–1.0	82	Dystric Epifibric Endocryic Histosols; Histic Reductaquic Turbic Cryosols (Loamic); Dystric Fibric Histosols (Gelic)
Khanymey, (Kh)	63.8	−5.6°C	540	Sand	peat mounds	0.1–1.4	90	Dystric Hemic Cryic Histosols; Spodic Histic Turbic Cryosols (Albic, Arenic); Histic Turbic Cryosols (Albic, Arenic)
					permafrost subsidences	0.7–1.1	165	Dystric Hemic Histosols (Gelic)
					hollows	0.4–1.1	215	Dystric Epifibric Histosols; Spodic Histic Turbic Cryosols (Arenic); Gleyic Histic Entic Podzols (Turbic)
Kogalum, (Kg)	62.3	−4.0°C	594	Sand	ridge	1.7–2.3	–	Dystric Ombric Fibric Histosols (Hyperorganic)
					hollows	1.0–1.5	–	Dystric Ombric Fibric Histosols

1027

1028

1029

1030

1031



1032

**Table 2.** Mean values of DOC, major and TE concentration with S.D. of elements in various microlandscape across the permafrost gradient. Concentrations of DOC, DIC, Cl<sup>-</sup>,

1033

SO<sub>4</sub><sup>2-</sup>, Ca, Mg, K, Al, Fe, Si, and Na are given in ppm and all other trace elements are in ppb.

Elements	Kogalym (62.259°N)		Khanymey (63.785°N)			Pangody (65.873°N)		Urengoy (66.085°N)			Tazovsky (67.367°N)			WSL-mean mound/ polygon	WSL mean hollow
	mound n=4	hollow n=2	mound n=20	hollow n=4	subsidence n=4	mound n=8	hollow n=4	mound n=3	hollow n=4	subsidence n=2	polygon n=12	hollow n=7	frost crack n=4		
DOC	50.56±15.6	33.7±4.1	82.9±29.7	49.6±13.5	76.5±21	90.2±55.3	81.58±15	74.28±25.2	50.2±3.64	97.9±19.9	72.9±12.9	52.53±7.7	58.4±30.8	79.8	58.1
DIC	1.45±0.27	1.42±0.3	1.65±0.36	1.42±0.05	1.7±0.11	1.84±0.35	1.54±0.46	1.36±0.17	1.58±0.7	1.32±0.17	1.44±0.18	1.68±0.13	1.76±0.42	1.59	1.56
Cl <sup>-</sup>	0.61±0.5	0.91±0.06	0.49±0.4	0.26±0.17	0.31±0.16	0.52±0.43	0.68±0.45	0.47±0.33	0.54±0.41	0.53±0.21	0.20±0.18	0.18±0.09	0.28±0.15	0.42	0.43
SO <sub>4</sub> <sup>2-</sup>	0.13±0.03	0.16±0.09	0.64±0.47	0.15±0.02	0.14±0.06	0.41±0.35	0.24±0.18	0.81±0.14	0.16±0.05	0.17±0.03	0.60±0.44	0.067±0.04	0.13±0.10	0.56	0.14
Ca	1.03±0.34	1.07±0.57	0.74±0.52	1.34±0.17	0.97±0.14	1.33±0.4	1.14±0.16	1.13±0.22	1.17±0.35	0.97±0.17	2.04±1.7	1.78±1.03	1.8±0.4	1.31	1.40
Mg	0.13±0.07	0.12±0.05	0.14±0.11	0.21±0.09	0.13±0.04	0.28±0.22	0.35±0.27	0.12±0.03	0.19±0.18	0.07±0.001	0.3±0.29	0.34±0.3	0.36±0.16	0.20	0.27
K	1.06±0.49	1.16±0.26	0.32±0.13	0.34±0.26	0.31±0.06	0.99±0.62	0.79±0.33	0.21±0.06	0.16±0.05	0.18±0.004	0.26±0.17	0.19±0.06	0.14±0.1	0.47	0.42
Al	0.13±0.06	0.15±0.03	0.19±0.12	0.26±0.04	0.20±0.05	0.39±0.26	0.67±0.33	0.31±0.15	0.18±0.05	0.17±0.03	0.41±0.3	0.37±0.22	0.42±0.22	0.28	0.35
Fe	1.17±1.04	0.96±0.6	0.54±0.42	0.76±0.21	0.85±0.19	1.97±1.05	1.99±1.23	0.90±0.04	1.54±0.6	0.87±0.13	1±0.73	1.14±0.65	2.19±0.97	0.99	1.28
Si	1.94±1.45	1.12±0.33	1.04±1.27	0.6±0.18	0.82±0.32	2.94±1.44	3.08±1.7	0.49±0.14	0.82±0.38	0.38±0.03	1.12±0.97	1.27±1.35	1.77±1.51	1.39	1.42
Li	0.46±0.04	0.63±0.10	0.45±0.42	0.39±0.05	0.40±0.20	1.14±0.76	1.11±0.63	0.17±0.01	0.37±0.36	0.17±0.01	0.36±0.15	0.80±0.71	0.44±0.25	0.53	0.68
B	1.39±0.57	3.39±0.07	4.09±2.02	2.97±0.97	2.91±1.99	2.19±1.29	2.03±1.16	0.63±0.34	N.D.	N.D.	3.54±1.52	1.31±0.71	2.38±0.85	3.26	2.13
Na	0.44±0.25	0.45±0.09	0.28±0.12	0.35±0.15	0.26±0.03	0.39±0.2	0.50±0.11	0.23±0.1	0.25±0.22	0.14±0.02	0.19±0.08	0.26±0.10	0.20±0.1	0.29	0.34
Ti	2.33±1.21	0.66±0.21	2.92±2.02	2.02±0.48	3.23±0.8	3.8±1.57	3.68±1.58	1.72±0.36	1.38±0.32	1.43±0.02	3.69±0.71	3.48±1.34	5.25±2.78	3.07	2.54
V	0.51±0.38	0.28±0.18	0.43±0.26	0.35±0.22	0.56±0.114	0.67±0.22	0.96±0.67	0.77±0.47	0.26±0.082	0.28±0.09	1.71±1.51	0.97±0.52	1.63±0.99	0.83	0.65
Cr	0.54±0.28	0.31±0.11	1.12±0.36	1.17±0.56	1.23±0.42	1.12±0.4	1.34±0.39	0.27±0.18	0.39±0.2	0.203±0.001	0.93±0.38	0.86±0.31	1.22±0.65	0.97	0.87
Mn	6.89±3.3	10.8±0.4	3.33±2.95	3.05±1.6	2.64±1.34	11.3±8.5	5.77±4.25	6.05±2.02	14.38±5.54	9.31±1.58	58.9±37.3	47.3±40.0	59.1±34.33	19.7	21.21
Co	0.18±0.04	0.16±0.12	0.22±0.11	0.29±0.1	0.34±0.09	1.18±0.54	1.24±0.65	0.26±0.09	0.34±0.14	0.21±0.03	0.99±0.63	0.92±0.62	1.43±0.46	0.59	0.677
Ga	0.05±0.04	0.02±0.01	0.51±0.45	0.06±0.02	0.55±0.44	0.07±0.03	0.15±0.15	0.59±0.22	0.42±0.18	0.32±0.01	0.20±0.18	0.31±0.23	0.51±0.42	0.32	0.224
As	1.00±0.49	0.76±0.2	0.53±0.31	0.96±0.3	0.74±0.32	0.83±0.6	1.07±0.86	0.2±0.06	0.17±0.06	0.105±0.075	1.12±0.98	0.96±0.37	1.90±0.89	0.76	0.796
Rb	0.93±0.53	0.35±0.2	0.48±0.36	0.62±0.31	0.47±0.46	0.72±0.58	0.33±0.17	0.23±0.22	0.27±0.15	0.056±0.035	0.37±0.28	0.56±0.50	0.53±0.26	0.52	0.454
Zr	0.10±0.10	0.02±0.001	0.21±0.23	0.13±0.06	0.24±0.15	0.33±0.23	0.56±0.3	0.14±0.06	0.19±0.2	0.066±0.050	0.54±0.45	0.34±0.15	0.53±0.24	0.304	0.281
Nb	0.01±0.005	0.003±0.002	0.013±0.009	0.017±0.009	0.011±0.003	0.021±0.01	0.026±0.016	0.004±0.002	0.004±0.001	0.004±0.000	0.018±0.012	0.012±0.005	0.02±0.01	0.014	0.013
Mo	0.037±0.02	0.084±0.08	0.09±0.07	0.129±0.09	0.11±0.01	0.082±0.06	0.075±0.036	0.028±0.016	0.028±0.008	0.024±0.004	0.064±0.021	0.054±0.021	0.12±0.08	0.075	0.070
Cd	0.19±0.035	0.4±0.18	0.34±0.54	0.42±0.42	0.56±0.5	0.27±0.27	0.13±0.04	0.040.019	0.025±0.008	0.008±0.004	0.067±0.065	0.04±0.027	0.09±0.07	0.223	0.161
Ni	1.04±0.76	0.55±0.24	0.92±0.48	1.51±0.62	1.22±0.62	3.29±1.26	3.12±1.32	1.43±0.7	1.25±0.45	1±0.14	2.9±1.95	2.12±0.95	3.53±1.54	1.89	1.859
Cu	4.44±2.7	2.21±0.48	5.36±3.74	1.62±0.14	4.27±3.46	5.02±3.7	5.78±3.95	6.02±4	5.41±2.24	1.82±0.23	5.86±3.1	4.05±3.05	2.33±0.95	5.39	4.000
Zn	9.97±6.7	12.48±0.5	7.97±4.47	10.16±6.4	10.03±6.67	8.14±5.4	3.51±0.49	8±5.38	6.34±2.04	1.76±0.11	6.34±3.32	7.88±3.46	5.77±0.36	7.75	7.626
Sr	5.37±1.05	4.46±3.03	7.62±4.42	8.15±2.94	7.87±1.08	10.95±2.98	10.7±5.35	5.9±2.3	6.5±3.6	4.32±0.15	13.1±9.02	8.41±3.49	11.7±4.22	9.42	8.312
Sb	0.06±0.04	0.05±0.01	0.05±0.03	0.06±0.02	0.042±0.016	0.05±0.03	0.037±0.011	0.013±0.012	0.013±0.004	0.004±0.001	0.032±0.01	0.025±0.012	0.032±0.01	0.044	0.034
Cs	0.032±0.03	0.02±0.016	0.036±0.028	0.03±0.02	0.04±0.03	0.023±0.02	0.018±0.01	0.004±0.002	0.006±0.004	0.003±0.001	0.012±0.013	0.006±0.007	0.056±0.03	0.025	0.015
Ba	22.5±9.3	18.87±9.57	35.7±20.6	33.57±22.24	32.5±17.7	22.7±13.2	38.8±17.7	18.76±6.89	13.83±6.35	10.8±0.6	16.77±6.85	16.30±5.82	14.99±9.11	26.23	23.64
La	0.24±0.19	0.15±0.04	0.37±0.33	0.25±0.17	0.26±0.06	0.348±0.208	0.502±0.277	0.354±0.26	0.14±0.07	0.112±0.05	0.34±0.17	0.23±0.10	0.40±0.22	0.346	0.261
Ce	0.51±0.47	0.22±0.11	0.67±0.51	0.53±0.44	0.54±0.09	0.725±0.484	1.039±0.536	0.66±0.53	0.29±0.136	0.236±0.1	0.74±0.35	0.51±0.21	0.87±0.58	0.685	0.543
Pr	0.03±0.02	0.015±0.014	0.082±0.06	0.059±0.057	0.066±0.014	0.08±0.06	0.114±0.05	0.05±0.034	0.028±0.013	0.022±0.01	0.094±0.05	0.06±0.032	0.108±0.073	0.079	0.059

Nd	0.257±0.2	0.088±0.04	0.33±0.26	0.26±0.21	0.27±0.06	0.34±0.22	0.383±0.097	0.194±0.13	0.115±0.054	0.086±0.037	0.407±0.24	0.24±0.13	0.43±0.28	0.338	0.233
Sm	0.028±0.01	0.01±0.0074	0.07±0.05	0.044±0.038	0.058±0.016	0.072±0.047	0.080±0.021	0.04±0.027	0.025±0.012	0.018±0.009	0.092±0.057	0.052±0.031	0.099±0.069	0.071	0.047
Eu	0.011±0.01	0.004±0.002	0.015±0.010	0.010±0.007	0.015±0.007	0.015±0.01	0.016±0.005	0.012±0.006	0.008±0.004	0.007±0.003	0.022±0.013	0.013±0.008	0.025±0.016	0.017	0.011
Gd	0.03±0.014	0.02±0.007	0.07±0.05	0.05±0.05	0.061±0.02	0.069±0.046	0.078±0.021	0.042±0.027	0.025±0.013	0.019±0.009	0.096±0.061	0.052±0.029	0.099±0.068	0.0721	0.049
Tb	0.007±0.006	0.003±0.001	0.014±0.004	0.007±0.006	0.009±0.003	0.01±0.007	0.012±0.004	0.006±0.004	0.003±0.002	0.003±0.001	0.014±0.01	0.0074±0.004	0.015±0.011	0.0123	0.007
Dy	0.04±0.04	0.017±0.002	0.061±0.05	0.041±0.034	0.05±0.016	0.055±0.037	0.081±0.04	0.031±0.02	0.018±0.009	0.016±0.009	0.078±0.05	0.0424±0.026	0.087±0.068	0.0608	0.042
Ho	0.008±0.007	0.003±0.001	0.011±0.008	0.011±0.01	0.009±0.003	0.011±0.007	0.012±0.003	0.007±0.004	0.004±0.002	0.004±0.002	0.016±0.011	0.009±0.005	0.018±0.014	0.0115	0.008
Er	0.021±0.019	0.0069±0.0057	0.030±0.021	0.023±0.022	0.03±0.01	0.031±0.021	0.034±0.009	0.017±0.01	0.012±0.008	0.009±0.004	0.047±0.035	0.0261±0.016	0.051±0.037	0.0330	0.022
Tm	0.0028±0.0025	0.0015±0.00001	0.005±0.004	0.0032±0.003	0.004±0.001	0.004±0.003	0.005±0.001	0.002±0.001	0.002±0.001	0.001±0.0004	0.007±0.005	0.0035±0.003	0.007±0.004	0.0047	0.003
Yb	0.0164±0.014	0.006±0.0047	0.021±0.014	0.018±0.018	0.022±0.009	0.026±0.017	0.029±0.007	0.014±0.008	0.012±0.01	0.007±0.004	0.043±0.032	0.0250±0.017	0.046±0.032	0.0271	0.020
Lu	0.0022±0.0018	0.0014±0.00001	0.0034±0.003	0.003±0.0025	0.003±0.001	0.004±0.002	0.004±0.001	0.002±0.001	0.002±0.001	0.001±0.0004	0.007±0.005	0.0036±0.003	0.006±0.004	0.0041	0.003
Hf	0.004±0.003	0.0013±0.0002	0.006±0.005	0.008±0.003	0.008±0.004	0.012±0.008	0.016±0.007	0.006±0.003	0.005±0.005	0.003±0.002	0.015±0.014	0.011±0.005	0.016±0.008	0.0095	0.009
W	0.028±0.02	0.01±0.0006	0.036±0.03	0.039±0.031	0.044±0.007	0.026±0.015	0.032±0.012	0.008±0.007	0.004±0.006	0.001±0.001	0.014±0.008	0.015±0.006	0.022±0.018	0.0262	0.020
Tl	0.011±0.008	0.005±0.003	0.007±0.004	0.005±0.004	0.007±0.002	0.008±0.004	0.009±0.007	0.001±0.001	0.002±0.001	0.0009±0.00	0.003±0.001	0.003±0.002	0.006±0.003	0.0059	0.005
Pb	1.24±0.64	0.59±0.06	1.08±0.71	1.03±0.47	0.90±0.25	0.70±0.32	0.777±0.22	0.49±0.42	0.27±0.13	0.13±0.0015	0.603±0.186	0.666±0.348	0.86±0.16	0.8636	0.674
Th	0.04±0.035	0.015±0.006	0.065±0.06	0.040±0.035	0.051±0.004	0.08±0.04	0.089±0.023	0.073±0.053	0.032±0.023	0.02±0.007	0.093±0.054	0.049±0.024	0.07±0.03	0.0740	0.049
U	0.02±0.018	0.014±0.008	0.0303±0.03	0.026±0.02	0.026±0.005	0.028±0.016	0.055±0.025	0.008±0.006	0.015±0.01	0.005±0.001	0.026±0.014	0.021±0.018	0.032±0.017	0.0265	0.026

1034

1035

1036

1037

Element	Habitat	Equation	$R^2$
S.C.	Hollow	[S.C.] = -2.367L + 207.36	0.15
	Mound/polygon	[S.C.] = -0.493L + 73.345	0.006
pH	Hollow	[pH] = 0.0278L + 2.4126	0.035
	Mound/polygon	[pH] = 0.0663L - 0.3568	0.515
DOC	Hollow	[DOC] = 4.6937L - 251.92	0.31
	Mound/polygon	[DOC] = 4.0364L - 188.61	0.29
SUVA	Hollow	[SUVA] = 0.148L - 6.861	0.599
	Mound/polygon	[SUVA] = 0.0258L + 1.192	0.031
DIC	Hollow	[DIC] = 0.0405L - 1.131	0.58
	Mound/polygon	[DIC] = 0.0191 L + 0.3357	0.1
Cl <sup>-</sup>	Hollow	[Cl <sup>-</sup> ] = -0.084L + 5.9763	0.33
	Mound/polygon	[Cl <sup>-</sup> ] = -0.0601L + 4.368	0.64
SO <sub>4</sub> <sup>2-</sup>	Hollow	[SO <sub>4</sub> <sup>2-</sup> ] = -0.0087L + 0.7179	0.079
	Mound/polygon	[SO <sub>4</sub> <sup>2-</sup> ] = 0.0824L - 4.8422	0.41
Ca	Hollow	[Ca] = 0.0612L - 2.6683	0.19
	Mound/polygon	[Ca] = 0.1828L - 10.639	0.59
Mg	Hollow	[Mg] = 0.0405L - 2.395	0.69
	Mound/polygon	[Mg] = 0.0302L - 1.773	0.43
Na	Hollow	[Na] = -0.0348L + 2.621	0.49
	Mound/polygon	[Na] = -0.0389L + 2.836	0.52
K	Hollow	[K] = -0.1488L + 10.224	0.47
	Mound/polygon	[K] = -0.1159L + 8.119	0.33
Al	Hollow	[Al] = 0.0555L - 3.3573	0.43
	Mound/polygon	[Al] = 0.0577L - 3.4737	0.91
Fe	Hollow	[Fe] = 0.1585L - 9.109	0.44
	Mound/polygon	[Fe] = 0.1399L - 7.934	0.3
Ti	Hollow	[Ti] = 0.462L - 27.841	0.52
	Mound/polygon	[Ti] = 0.172L - 8.3533	0.19
Mn	Hollow	[Mn] = 5.6454L - 351.11	0.41
	Mound/polygon	[Mn] = 7.6632L - 481.39	0.44
Co	Hollow	[Co] = 0.1618L - 9.9304	0.51
	Mound/polygon	[Co] = 0.1658L - 10.218	0.5
Ni	Hollow	[Ni] = 0.3096L - 18.437	0.43
	Mound/polygon	[Ni] = 0.4012L - 24.19	0.55
Cu	Hollow	[Cu] = 0.6695L - 39.754	0.54
	Mound/polygon	[Cu] = 0.2503L - 10.948	0.63
Zn	Hollow	[Zn] = -1.2677L + 90.571	0.56
	Mound/polygon	[Zn] = -0.5584L + 44.424	0.78
V	Hollow	[V] = 0.1308L - 7.9299	0.56
	Mound/polygon	[V] = 0.2026L - 12.383	0.6
Ga	Hollow	[Ga] = 0.0686L - 4.275	0.68
	Mound/polygon	[Ga] = 0.0207L - 1.0605	0.03
Rb	Hollow	[Rb] = -0.0229L + 1.939	0.11
	Mound/polygon	[Rb] = -0.096L + 6.7962	0.48
Cs	Hollow	[Cs] = -0.0036L + 0.2517	0.39
	Mound/polygon	[Cs] = -0.0052L + 0.361	0.62
Sr	Hollow	[Sr] = 0.7681L - 42.186	0.45
	Mound/polygon	[Sr] = 1.2825L - 74.614	0.69
Zr	Hollow	[Zr] = 0.0714L - 4.399	0.49
	Mound/polygon	[Zr] = 0.0664L - 4.0544	0.57
Mo	Hollow	[Mo] = -0.0116L + 0.8297	0.4
	Mound/polygon	[Mo] = 0.0011L - 0.0092	0.01
Sb	Hollow	[Sb] = -0.0068L + 0.4819	0.53
	Mound/polygon	[Sb] = -0.0069L + 0.489	0.54
Cd	Hollow	[Cd] = -0.0919L + 6.1957	0.79
	Mound/polygon	[Cd] = -0.0402L + 2.8027	0.4
La	Hollow	[La] = 0.0228L - 1.224	0.11
	Mound/polygon	[La] = 0.0163L - 0.728	0.42
Ce	Hollow	[Ce] = 0.0675L - 3.873	0.19

	Mound/polygon	[Ce] = 0.0387L - 1.8553	0.76
Sm	Hollow	[Sm] = 0.0077L - 0.4591	0.34
	Mound/polygon	[Sm] = 0.0084L - 0.4861	0.43
Eu	Hollow	[Eu] = 0.0017L - 0.1001	0.56
	Mound/polygon	[Eu] = 0.0015L - 0.0848	0.52
Gd	Hollow	[Gd] = 0.0054L - 0.3021	0.24
	Mound/polygon	[Gd] = 0.0094L - 0.5536	0.47
Pr	Hollow	[Pr] = 0.008L - 0.4652	0.18
	Mound/polygon	[Pr] = 0.0084L - 0.4788	0.46
Dy	Hollow	[Dy] = -0.0003L + 0.0475	0.0004
	Mound/polygon	[Dy] = -0.0057L + 0.41	0.4
Yb	Hollow	[Yb] = 0.0032L - 0.189	0.49
	Mound/polygon	[Yb] = 0.0038L - 0.2209	0.45
Lu	Hollow	[Lu] = 0.0004L - 0.0202	0.39
	Mound/polygon	[Lu] = 0.0006L - 0.0349	0.44
W	Hollow	[W] = -0.0015L + 0.1214	0.049
	Mound/polygon	[W] = -0.0038L + 0.2672	0.47
Tl	Hollow	[Tl] = -0.0004L + 0.0327	0.11
	Mound/polygon	[Tl] = -0.0015L + 0.1056	0.66
Hf	Hollow	[Hf] = 0.0019L - 0.1135	0.47
	Mound/polygon	[Hf] = 0.002L - 0.1187	0.68
Pb	Hollow	[Pb] = -0.0438L + 3.5297	0.12
	Mound/polygon	[Pb] = -0.1482L + 10.465	0.87
Th	Hollow	[Th] = 0.0078L - 0.4603	0.34
	Mound/polygon	[Th] = 0.0095L - 0.5465	0.92
U	Hollow	[U] = 0.0021L - 0.1101	0.065
	Mound/polygon	[U] = -0.0004L + 0.047	0.01

1040

1041

1042

1043

1044

1045

1046

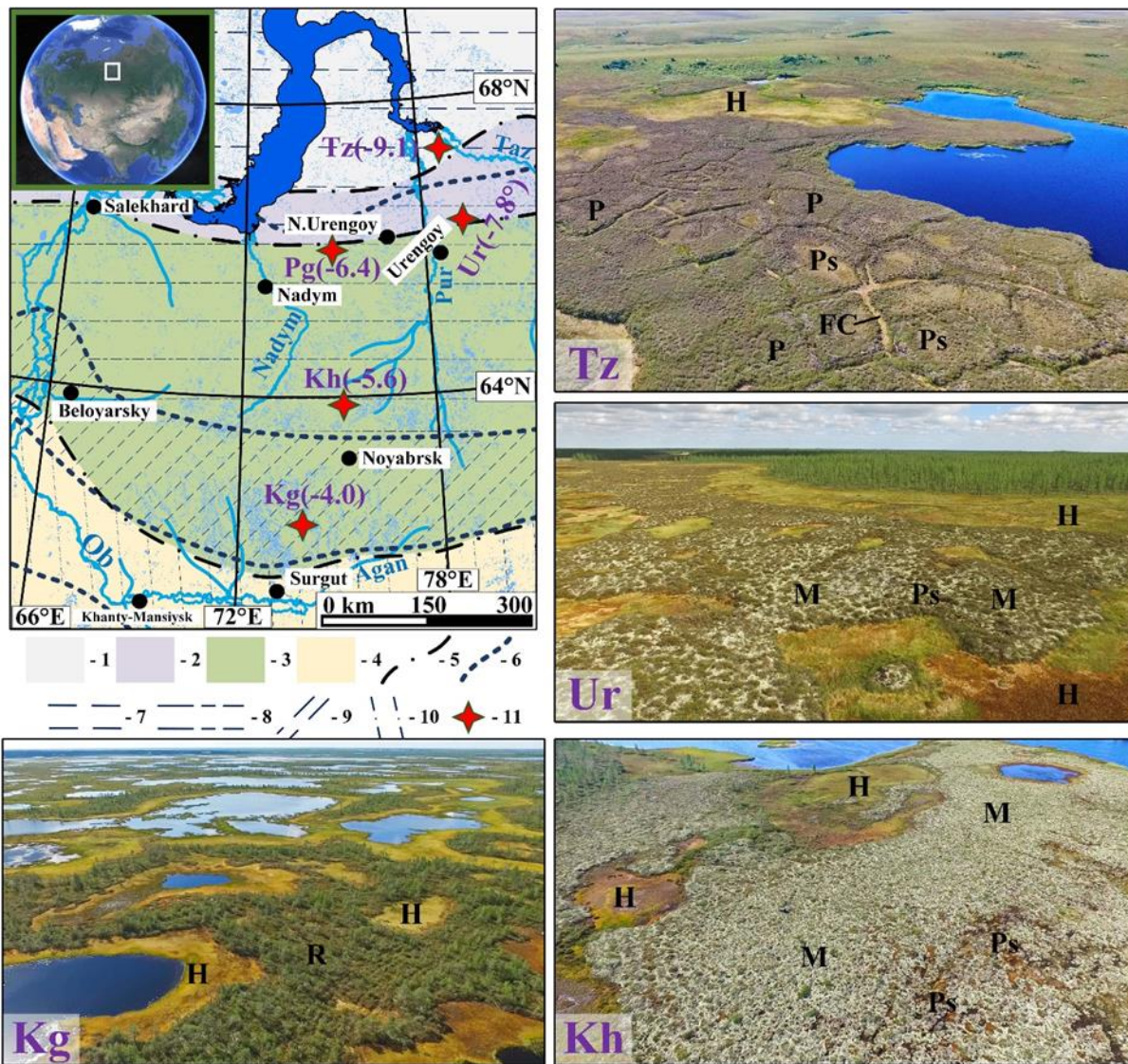
1047

1048

1049

1050

1051



1052

1053

1054

1055

1056

1057

1058

1059

1060

1061

1062

1063

1064

1065

**Figure 1.** Map of the study site with permafrost boundaries (Brown et al., 2001; <http://portal.intermap.com> (NSIDC)), with 5 main test sites: Kogalym (Kg), Khanymey (Kh), Pangody (Pg), Urengoy (Ur) and Tazovsky (Tz). The mean annual temperatures are given in parenthesis. The inserts represent aerial (drone-made) photos of main sites with the position of mound/polygon (M/P), hollow (H), frost crack (FC) and permafrost subsidence (Ps). On the Kogalym site, a hollow (H) – ridge (R) – lake complex is a dominating landscape type.

The numbers on the legend represent the following: 1, tundra; 2, forest-tundra; 3, northern taiga; 4, middle taiga; 5, borders between natural biomes; 6, borders between permafrost zones; 7, continuous permafrost; 8, discontinuous permafrost; 9, sporadic permafrost; 10, isolated permafrost; 11, key study sites with mean annual temperature in the parentheses.

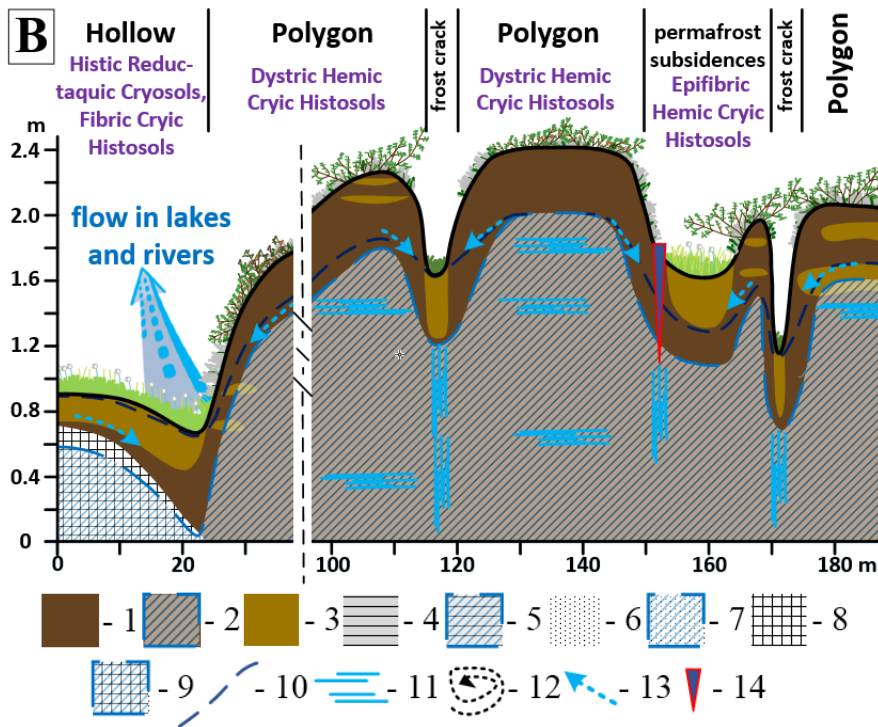
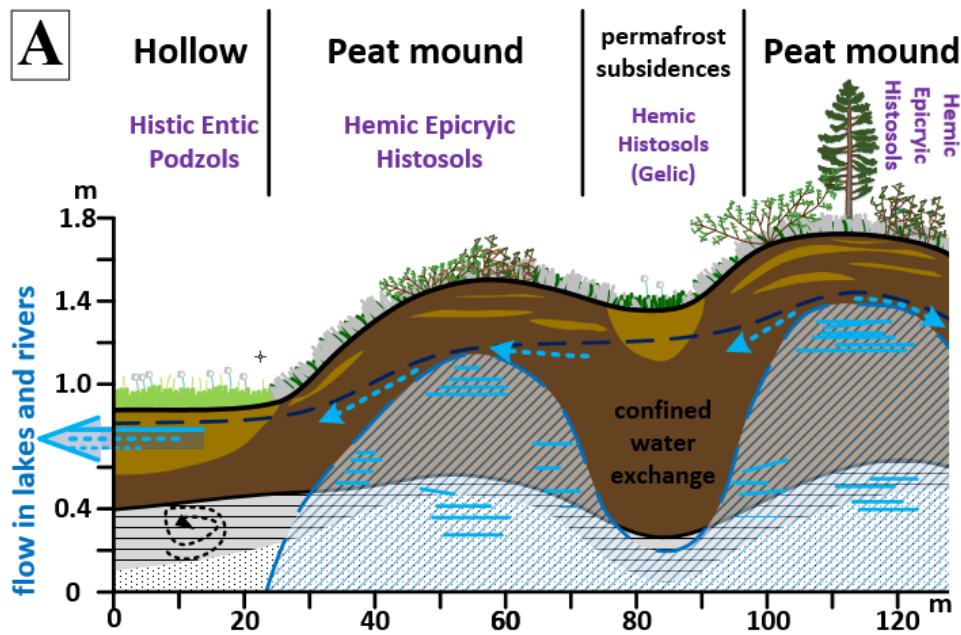


**Figure 2.** Soil transect of typical bog microlandscapes of flat mound palsa (A) and polygonal frozen bog (B). This vertical line in B indicates a discontinuity of hydrological flow-path. The numbers on the legend represent the following: 1, moss-lichen-sedge peat of medium degree of decomposition (Hemic); 2, permanently frozen peat; 3, moss-based peat of low degree of decomposition; 4, illuvial-Fe-humic (spodic) horizon; 5, permanently frozen spodic horizon; 6, sand and silt deposits; 7, frozen sand and silts; 8, heavy clay deposits; 9, frozen clays; 10, the level of suprapermafrost waters in August; 11, ice wedges; 12, cryoturbation features in soil; 13, the direction of soil water transport, typically along the permafrost boundary; 14, small crack on the polygonal bog.

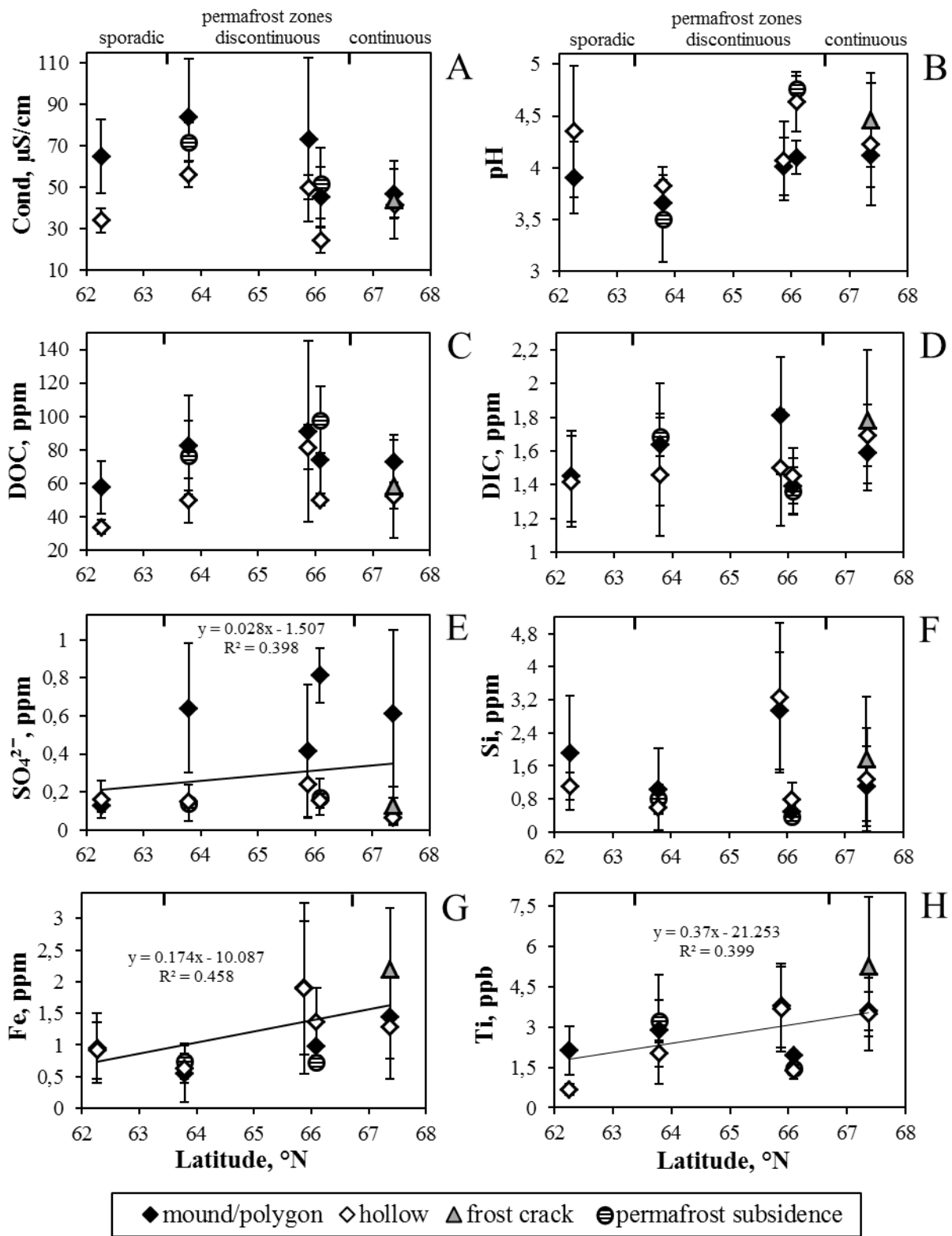


**Figure 3.** Mean values of Specific conductivity (A), pH (B), DOC (C), DIC (D),  $\text{SO}_4^{2-}$  (E), Si (F), Fe (G) and Ti (H) concentration in peat porewaters of the WSL as a function of latitude for mound and polygons (solid diamonds), hollow (open diamonds), frost crack (grey triangles) and permafrost subsidence/depression (hatched circles). The solid line is a linear fit to all data with the regression equation given on each graph.

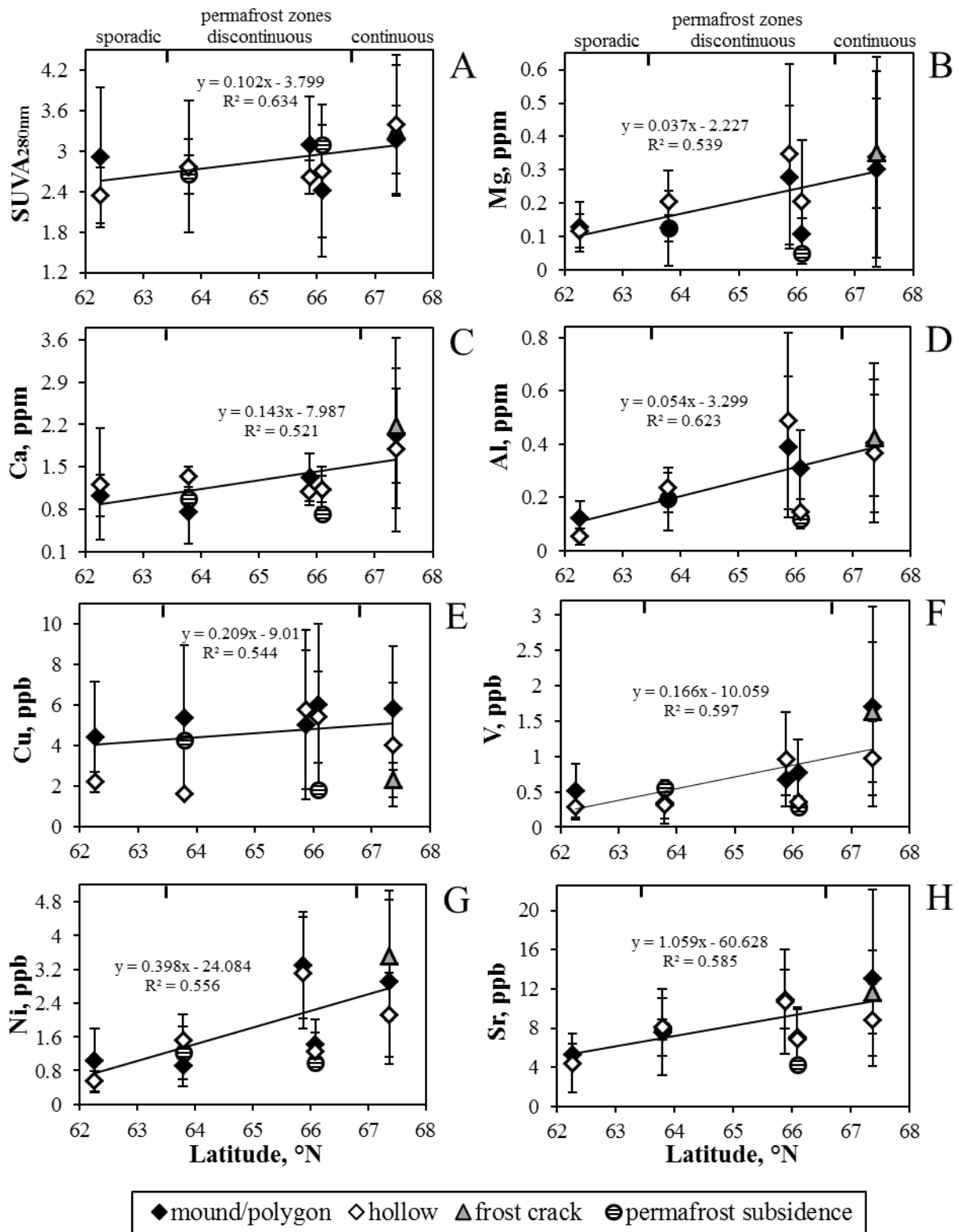


**Figure 4.** Mean values of SUVA<sub>280</sub> (A), Mg (B), Ca (C), Al (D), Cu (E), V (F), Ni (G), Sr (H) concentration in peat porewaters of the WSL as a function of latitude for mound and polygons (solid diamonds), hollow (open diamonds), frost crack (grey triangles) and permafrost subsidence/depression (hatched circles). The solid line is a linear fit to all data with the regression equation given on each graph.



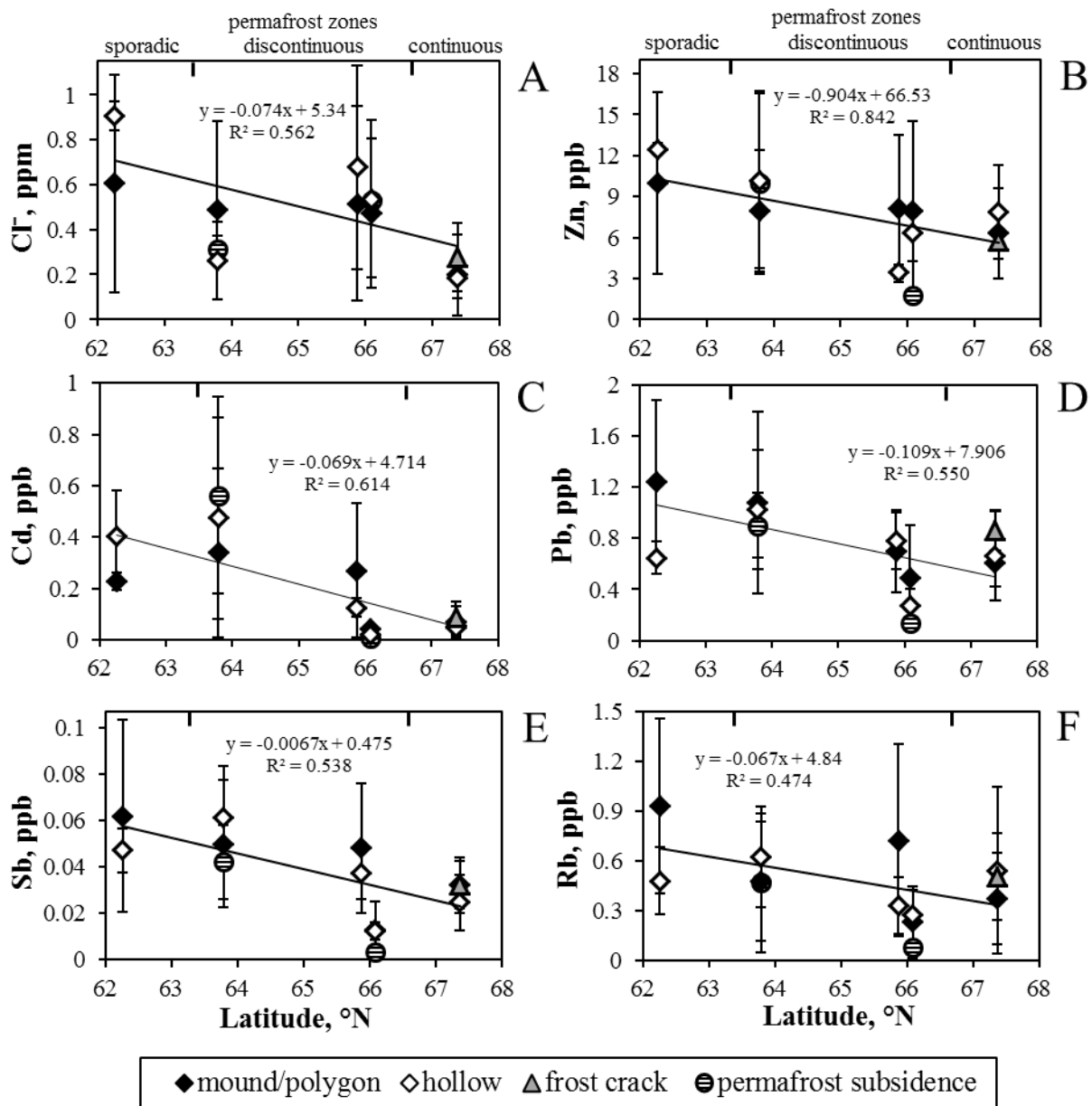


**Figure 5.** Mean concentrations of Cl (A), Zn (B), Cd (C), Pb (D), Sb (E), and Rb (F) in peat porewaters of the WSL as a function of latitude for mound and polygons (solid diamonds), hollow (open diamonds), frost crack (grey triangles) and permafrost subsidence/depression (hatched circles). The solid line is a linear fit to all data with the regression equation given on each graph.